Received 2 September 2023; revised 4 October 2023; accepted 18 October 2023. Date of publication 24 October 2023; date of current version 8 November 2023.

*Digital Object Identifier 10.1109/OJCOMS.2023.3327211*

# Artificial Intelligence in Visible Light Positioning for Indoor IoT: A Methodological Review

**VASILEIOS P. REKKAS[1] (Graduate Student Member, IEEE), LAZAROS ALEXIOS ILIADIS[1] (Graduate Student Member, IEEE), SOTIRIOS P. SOTIROUDIS[1], ACHILLES D. BOURSIANIS[1] (Member, IEEE), PANAGIOTIS SARIGIANNIDIS[2] (Member, IEEE), DAVID PLETS[3] (Member, IEEE), WOUT JOSEPH[3] (Senior Member, IEEE), SHAOHUA WAN[4] (Senior Member, IEEE), CHRISTOS G. CHRISTODOULOU[5] (Life Fellow, IEEE), GEORGE K. KARAGIANNIDIS[6,7] (Fellow, IEEE), AND SOTIRIOS K. GOUDOS[1,8] (Senior Member, IEEE)**

[1]ELEDIA@AUTH, School of Physics, Aristotle University of Thessaloniki, 541 24 Thessaloniki, Greece

[2]Department of Electrical and Computer Engineering, University of Western Macedonia, 501 00 Kozani, Greece

[3]imec-WAVES Group, Department of Information Technology, Ghent University, 9052 Ghent, Belgium

[4]Shenzhen Institute for Advanced Study, University of Electronic Science and Technology of China, Shenzhen 518110, China

[5]Department of Electrical and Computer Engineering, The University of New Mexico, Albuquerque, NM 87131, USA

[6]Department of Electrical and Computer Engineering, Aristotle University of Thessaloniki, 541 24 Thessaloniki, Greece

[7]Cyber Security Systems and Applied AI Research Center, Lebanese American University, Beirut 1102 2801, Lebanon

[8]Department of Electronics and Communication Engineering, Bharath University, Chennai 600073, India

CORRESPONDING AUTHOR: S. K. GOUDOS (e-mail: sgoudo@physics.auth.gr)

This work was supported by the Hellenic Foundation for Research and Innovation (HFRI) under the 3rd Call for HFRI Ph.D. Fellowships under Grant 6646.

**ABSTRACT** Indoor communication and positioning are significant fields of applications for indoor Internet of Things (IoT) given the rapid growth of IoT in smart cities, smart grids, and smart industries. Visible light positioning (VLP) has become more and more attractive for researchers to provide indoor location-aware IoT services. Additionally, artificial intelligence (AI) has attracted considerable research effort to address the challenges in visible-light communication (VLC) systems. This is an emerging technology in next-generation wireless networks. However, despite the rapid progress, the use of AI in localization, navigation, and position estimation is still underexplored in VLC systems, and various research challenges are still open. This methodological review summarizes the research efforts regarding the use of AI in the field of VLP, to improve the position estimation accuracy in both two-dimensional (2D) and three-dimensional (3D) indoor IoT applications. This treatise also presents open issues and potential future directions for motivating further research in the field. Various databases were utilized in this paper: Scopus, Google Scholar, and IEEE Xplore; obtained 88 papers from 2017 to early 2023. Most (68%) of the AI articles in VLP systems are machine learning (ML) methods applied for localization and position estimation in VLC systems, while the other 32% of the research articles focussed on evolutionary algorithms. ML and evolutionary models may present limitations in terms of complexity and time-consuming nature but offer highly accurate, robust, reliable, and cost-effective results in terms of position estimation over conventional approaches.

**INDEX TERMS** Artificial intelligence, indoor localization, machine learning, evolutionary algorithms, visible light communication, visible light positioning.

## I. INTRODUCTION

THE INTERNET of Things (IoT) has emerged as a vision for future networks through the realization of smart manufacturing, smart grid, and smart city [1], [2], [3]. However, with the advancement of wireless communication, an increasing number of smart devices are incorporated into the IoT, resulting in a shortage of radio frequency (RF) spectrum. In addition, certain indoor IoT devices require precise positioning, but multipath reflections and shadowing reduce the accuracy and dependability of indoor RF-based localization systems [4], [5].

Indoor location-based services (LBSs) have attracted considerable research effort, thanks to the plethora of possible use case scenarios; from smart home applications and service robots to large facility mapping and patient tracking in hospitals [6]. The rapid progress of IoT provides access to a large number of sensors and devices, opening great research opportunities for indoor positioning systems (IPSs) [7].

The need for accurate indoor localization technologies arises from the fact that the most prominent, for outdoor navigation and localization scenarios, global positioning system (GPS) technology is heavily degraded in indoor scenarios. GPS estimation accuracy drops significantly in such environments due to weak received signal strength (RSS), multi-path effects, and the inability to penetrate the building walls thoroughly [8].

Several competing technologies have been developed for the various use cases, as the complexity of indoor scenarios and LBSs makes it rather hard to find a single prevalent and robust technology for localization and positioning. Although wireless local area networks (WLANs), ultra-wideband (UWB), Zigbee, and Bluetooth have been frequently utilized, they are not only susceptible to electromagnetic signal interference generated by other RF wireless devices, but also require additional infrastructure. In addition, their deployment is rather complex and expensive [9].

Visible light communication (VLC), also known as optical wireless communication, emerges as a promising technology for accurate indoor position estimation in forthcoming wireless networks [10]. Visible light positioning (VLP) is a VLC-based technology that has gained a lot of attention as a promising solution, as it provides higher accuracy results for IPSs, compared to other technologies [11]. A comparison among the techniques for indoor localization [12], [13] can be summarized in Table 1.

VLP systems provide simultaneous communication and illuminance services, with high-speed data packets being transmitted using the visible light spectrum. In such configurations, light emitting diodes (LEDs) are the transmitters, and photo-detectors (PDs) are the receivers [14]. LEDs are power-efficient, cost-effective, have high bandwidth, and have a long lifespan [15]. VLP technology is immune to electromagnetic interference and can benefit from the free and unrestricted visible light portion of the spectrum, but the line-of-sight (LOS) is a mandatory condition [16]. Fig. 1 summarizes the major advantages and limitations of the VLP systems. Conventional VLP methods can provide accurate positioning in indoor environments, but still suffer from various types of noise (i.e., dark, shot, and thermal noise), and disturbance of the signal wave in the physical environment [17]. Artificial intelligence (AI) and machine learning (ML) approaches can learn the underlying physical model by observing a training dataset, and provide highly accurate position estimation, with respect to the computation time, thus greatly enhancing the performance of IPSs. As conventional methods struggle to provide accurate localization and position estimation, with respect to the computation time, AI algorithms can improve the performance and computational complexity of IPSs.

**TABLE 1.** Comparison of wireless indoor localization techniques.

| Tech. | Interf. | Cost | Power Consump. | Range |
|---|---|---|---|---|
| UWB | Immune | High | Medium | Short |
| Zigbee | RF | Medium | High | Long |
| Bluetooth | RF | Medium | Low | Short |
| Vis. Light | Light | Medium | Low | Short |

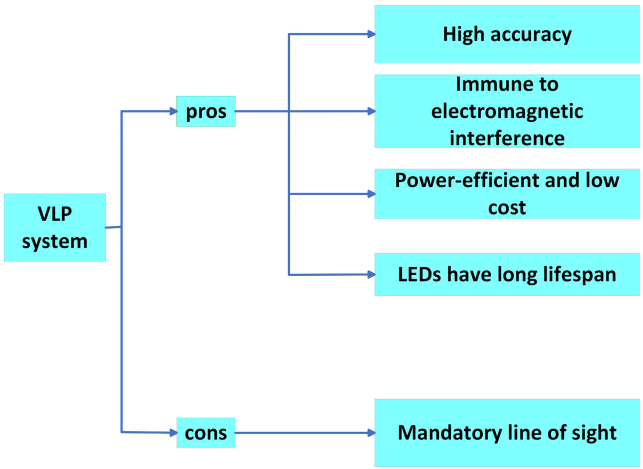


**FIGURE 1.** Advantages and limitations of VLP systems.

### A. RELATED WORK

AI methodologies have made substantial progress in recent years. The need to develop accurate VLP systems has sparked interest in the application of AI methods in VLP for indoor IoT networks. Additionally, ML and evolutionary positioning approaches have been established in the VLC community. VLP technology has received much attention, and as a result, there have been several reviews on the topic in a wider context of describing the structure of VLP models and common positioning methods.

In [18] authors present a thorough investigation of LED-based IPSs on positioning techniques, channel model information, and receiver design. The work presented in [19] examines the essential features of positioning systems based on VLC LED technology, with a particular emphasis on evaluating the precision of the experimental location estimation.

The survey in [7], thoroughly examines positioning systems that use non-RF solutions, such as those based on visible light localization, to develop unobtrusive passive systems. Reference [20] provides an overview of VLP and infrared light positioning (IRLP) systems, along with a comparison with conventional optical positioning systems. In [12], authors present some common processes and application scenarios in VLP systems, together with a detailed comparison with other wireless positioning systems. The study in [13] contains description requirements, specifications, advantages, and limitations for various indoor localization techniques, including VLP and wireless technologies. However, none of the previous review articles examines ML and meta-heuristic-empowered VLP approaches for indoor positioning estimation. Only in [21], does Tran and Ha summarize and evaluate the ML techniques that have been applied in VLP systems but do not take into account the evolutionary approach. Furthermore, the literature discussion needs an update, since the presented works in [21] range in the 2016-2020 period.

To the best of our knowledge, this is the first survey in the academic and industrial literature that explores and evaluates the influence of both ML and evolutionary methods in the field of localization and position estimation in VLC IPSs.

### B. MOTIVATION AND CONTRIBUTIONS

The oncoming IoT networks require highly accurate, robust, and cost-effective IPSs. Therefore, their design presents an important challenge for the research community. Despite the existence of various VLP systems and the substantial progress of AI, no work explores their combination in detail. AI techniques have the potential to enhance the efficiency and computational intricacy of localization in VLC systems compared to conventional methods. The purpose of this study is to highlight the scope of ML and evolutionary methodology in VLP systems, as well as to summarize open challenges and offer future directions in the field. The current study is more inclusive in the breadth of AI-empowered solutions in the localization of VLC IPSs. The main contributions of this work are as follows.

1) The main challenges of localization and positioning in indoor VLC systems are presented.
2) A thorough review of AI-empowered methods in VLP systems is discussed. In particular, the different state-of-the-art (SOTA) ML and evolutionary methodologies that are utilized in VLC IPSs, are presented and analyzed.
3) Open challenges and potential future trends are discussed to motivate academia and industry to explore the field.

## NOMENCLATURE

| | |
|---|---|
| 1D | One dimensional |
| 2D | Two dimensional |
| 3D | Three dimensional |
| AC | Actor-Critic |
| ACO | Ant colony optimization |
| Ada-XCoR | Co-training regression and adaptive boosting |
| AEs | Auto-encoders |
| AFSA | Artificial fish swarm algorithm |
| AI | Artificial intelligence |
| ANN | Artificial neural networks |
| ANs | Artificial Neurons |
| AoA | Angle of arrival |
| AP-PSO | Adaptive parameter PSO |
| AP-PSO-M | Adaptive mutation parameter PSO |
| BA | Bat algorithm |
| BP | Back-propagation |
| BR-DNN | Bayesian regularization deep neural network |
| CNNs | Convolutional neural networks |
| CPSO | Chaotic PSO |
| CSAE | Convolutional stacked auto-encoder |
| DBSCAN | Density-based spatial clustering of applications with noise |
| DE | Differential evolution |
| DL | Deep learning |
| DLSTM | Deep learning long short-term memory |
| DTs | Decision Trees |
| EAs | Evolutionary algorithms |
| ELM | Extreme learning machine |
| FNNs | Fully connected feed-forward neural networks |
| GA | Genetic algorithm |
| GANs | Generative adversarial networks |
| GD-LS | Grid-dependent least square |
| GGD | Generalized Gaussian distribution |
| GP | Gaussian process |
| GPS | Global positioning system |
| GRU | Gated recurrent unit |
| GWO | Grey wolf optimization |
| IHBA | Improved hybrid bat algorithm |
| IACS | Improved adaptive cuckoo search algorithm |
| IGA | Improved genetic algorithm |
| IHBA | Improved hybrid bat algorithm |
| IPSO | Improved PSO |
| IIPSO | Improved Immune PSO |
| IoT | Internet of Things |
| IPSO | Improved PSO |
| IPSs | Indoor positioning systems |
| IPWRL | Iterative point-wise reinforcement learning |
| IRLP | Infrared light positioning |
| IWOA | Improved whale optimization algorithm |
| kNN | k-nearest neighbor |
| LBSs | Location-based services |
| LED | Light-emitting diode |
| LoS | Line-of-sight |
| LR | Linear regression |
| LSE | Least square estimator |
| LSTM | Long Short-term Memory network |
| M-ANN | Memory-artificial neural network |
| MEX | Method of exhaustion |
| MFOA | Modified fruit fly optimization algorithm |

| | |
|---|---|
| MGA | Modified genetic algorithm |
| MIMO | Multiple-input-multiple-output |
| ML | Machine learning |
| MLP | Multilayer perceptron |
| MMBP | Modified momentum back-propagation |
| MRR | Maximum received recognition |
| MTL | Multi-task learning |
| N/A | Not available |
| NSGA-III | Non-sorting genetic algorithm III |
| okNN | Optimum k-nearest neighbors |
| PASS | Particle-assisted stochastic search |
| PD | Photo-detector |
| PE-DNN | Position-estimation deep neural network |
| PG | Policy gradient |
| PSD | Position-sensitive detector |
| PSO | Particle swarm optimization |
| ReLU | Rectified linear unit |
| ResNet | Residual neural network |
| RaF | Random forest |
| RF | Radio frequency |
| RL | Reinforcement learning |
| RNNs | Recurrent neural networks |
| RR | Ridge regression |
| RSS | Received signal strength |
| SAE | Stacked auto-encoder |
| SA-PSO | Simulated annealing PSO |
| SIAs | Swarm intelligence algorithms |
| SL | Supervised learning |
| SNR | Signal-to-noise-ration |
| SOTA | State-of-the-art |
| SPAO | Simultaneous positioning and orientating |
| STBC | Space-time block coding |
| SVM | Support vector machine |
| SVR | Support vector regressor |
| TDoA | Time difference of arrival |
| TLFN | Two layer-fusion network |
| ToA | Time of arrival |
| TS | Tabu search |
| TSNN | Two-stage neural network |
| UL | Unsupervised learning |
| UWB | Ultra wide-band |
| VLC | Visible light communication |
| VLP | Visible light positioning |
| wCkNN | Weight coefficients K-nearest neighbors |
| wkNN | Weighted K-nearest neighbors |
| WLANs | Wireless area networks |
| WokNN | Weighted optimum K-nearest neighbors |

The remainder of this paper is organized as follows. The research methodology is presented in Section II, while Section III analyzes the conventional VLP approaches and their challenges. In Section IV the AI-based results are presented and discussed. Finally, Section V highlights open challenges and future directions in the field, along with some conclusions.

*Notation:* In this work, we use lowercase Latin letters for scalars, while matrices are denoted with capital bold letters, i.e., **H**, and vectors with lowercase bold vectors, i.e., **x**.

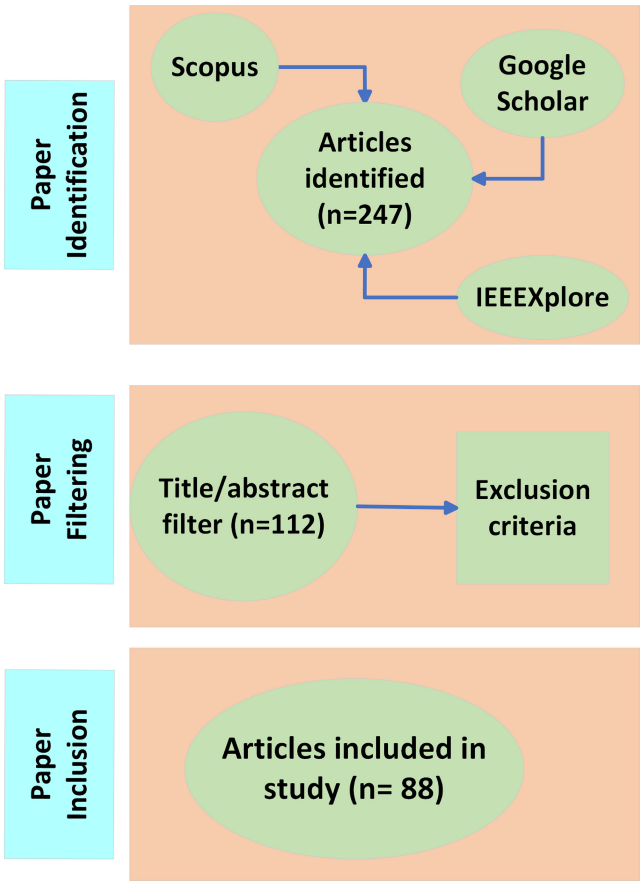


FIGURE 2. Strategy of paper inclusion procedure.

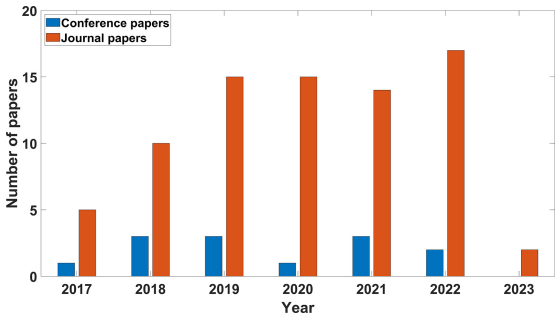


FIGURE 3. Distribution of journal articles and conference papers.

## II. METHODOLOGY

This treatise adopted a methodological review approach to process the literature on ML and metaheuristic enabled VLC systems for position and localization estimation, from 2017 to early 2023. The selection of relevant studies and the inclusion stages in this methodological review was conducted through a comprehensive literature search of the Scopus, GoogleScholar, and IEEE Xplore databases.

Fig. 2 illustrates the search strategy of the study. Fig. 3 demonstrates the distribution of journal articles and conference papers that were included in this review.

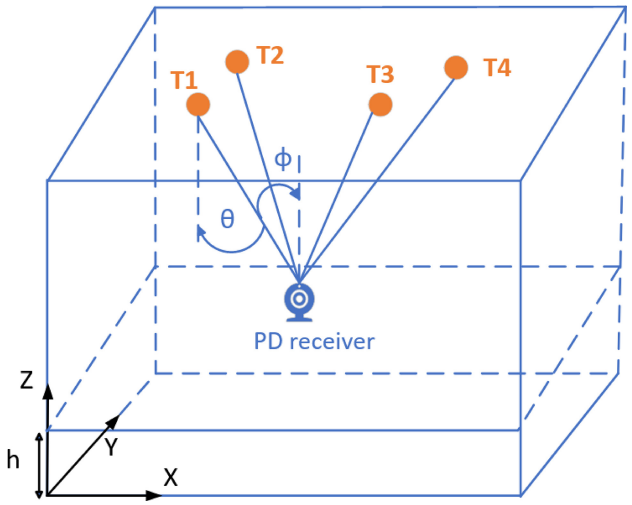


FIGURE 4. Visible light positioning system model.

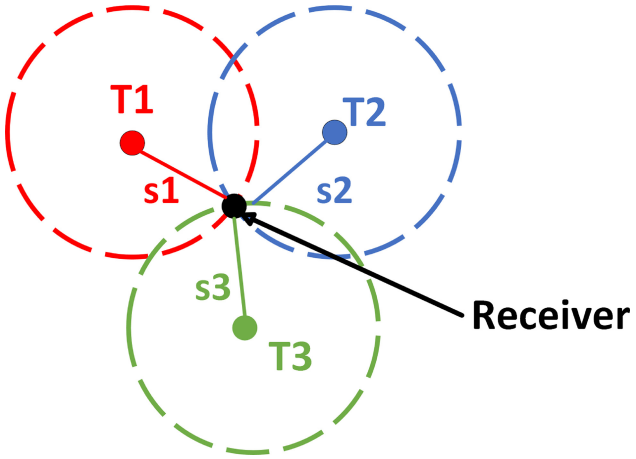


FIGURE 5. Trilateration operation diagram.

## III. CONVENTIONAL VLP METHODS AND CHALLENGES

In this Section, the conventional VLP techniques and their limitations are discussed.

### A. VLP METHODS

LED-based VLP technology can offer a vast number of indoor localization and navigation services in IoT applications, such as health centers, manufacturing robots, etc. Several VLC signal features have been developed to accurately estimate the indoor position coordinates, such as angle of arrival (AoA), time of arrival (ToA), time difference of arrival (TDoA), and RSS. AoA can provide highly accurate estimations but is rather complex, as the orientation of the receiver is important. ToA necessitates precise synchronization between transmitting and receiving devices, resulting in higher cost [16].

TDoA requires strict synchronization between the LEDs only [16], [22]. Moreover, distance estimation in indoor scenarios is usually limited [16].

Based on these signal features, various techniques have been developed for localization and position estimation of the receiver's coordinates in VLC systems, such as triangulation, lateration, proximity- and fingerprint-based methods. At least one of these approaches should be applied to a VLC system to accurately estimate the receiver's position.

A typical LED-based VLP formulation is depicted in Fig. 4. T1-T4 represent the LED sources, with the photodiode receiver recording the received light intensity waveform. Thanks to LEDs T1-T4 typically being modulated at specific frequencies (e.g., Pulse Width Modulation), it is possible at the receiver to demultiplex the contributions of each of the LEDs, allowing to combine the LEDs' RSSs, AoAs, or signal travel times to infer a position, depending on the used localization approach. In RSS-based VLP, the observed light intensity from each LED is converted to an estimated distance, based on an assumed light propagation model. In the case of AoA, usually, a multi-PD receiver structure is used, allowing to estimate the angle of incidence on the PD structure, from each of the LEDs. Timing-based approaches require a form of synchronization between the LEDs or between the LED and the receiver. The most prominently used techniques in VLP are described in more detail in the following sections.

#### 1) MULTILATERATION-TRILATERATION

Multilateration is a positioning method in which the target location is determined by measuring the distance from three or more reference transmitters. Should three transmitters be used to estimate the position of the receiver, then it is regarded as the trilateration method. Increasing the number of transmitters can enhance the precision of the positioning system, at the cost of complexity. To determine the receiver's location, intersecting circles are used in a multilateration system, with the radius of the circles corresponding to the distance between the transmitters and the receiver. The intersecting point corresponds to the position of the receiver [12].

For the trilateration approach, in a 3D environment considering the distances between the transmitters and the receiver can be found using RSS values or the distance differences utilizing TDOA, the position of the receiver can be found by solving the following equations for the transmitters $T_1$, $T_2$, and $T_3$ [23]:

$$(x - x_i)^2 + (y - y_i)^2 + (z - z_i)^2 = s_i^2 \; i \in 1, 2, 3 \qquad (1)$$

$[x_i, y_i, z_i]$ being the coordinates of the three LEDs, $s_i$ the distances between the LEDs and the receiver, and $(x, y, z)$ the position of the receiver. Fig. 5 demonstrates a typical system design utilizing the trilateration principles, to estimate the position of the receiver based on three transmitters $T_1$, $T_2$, and $T_3$.

#### 2) TRIANGULATION

Triangulation is a localization technique that utilizes the geometrical properties of triangles to estimate the distance

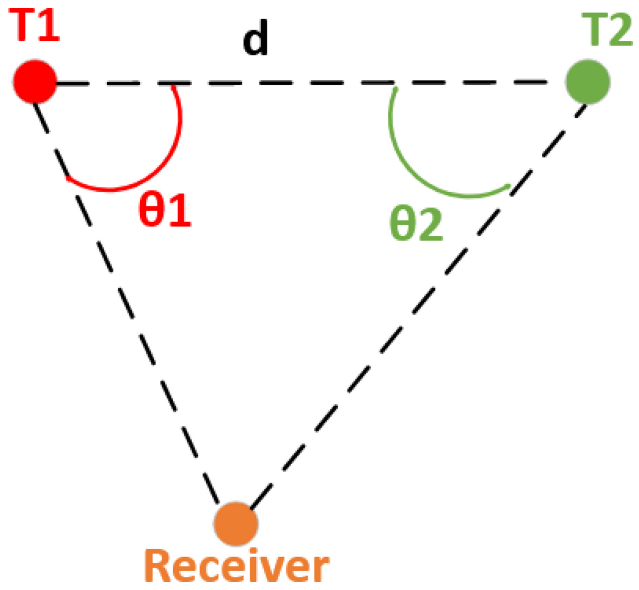


FIGURE 6. Triangulation operation diagram.

of the target. Considering that the measurement points are fixed and known, the position of the receiver can be inferred from the distance or received angle by taking into account the geometric features of triangles. A representation of the triangulation technique for a 2D environment is illustrated in Fig. 6.

#### 3) PROXIMITY

The proximity-based method can provide semantic location information of the target, with a simple implementation; When the target receives signals from known transmitter positions, it is deemed to be in close proximity to them. It is assumed that the transmitter from which the most powerful signal is received is the one located closest to the target, and its position is considered an approximate estimation of the target's position. If the signal intensity is the same from multiple transmitters, the target is assumed to be situated in the center of these transmitters. The proximity-based method is not very accurate since it is based on the density of the signal distribution [24].

#### 4) FINGERPRINTS

The location of the target is estimated in the fingerprint-based method by calculating real-time measurements and comparing them with offline fingerprints. RSS fingerprint method has gained a lot of momentum as a promising candidate in VLP systems, due to its simplicity, high accuracy, and affordability. In an RSS-based VLP system, a PD is used to detect RSS values from various LEDs. The distance between the transmitter and the receiver can be obtained by analyzing the received signal amplitudes or powers. When the distance between transmitters and receivers increases, the received measured power decreases. Therefore, RSS-based VLP can accurately estimate the desired distance. The RSS measurements are given with unknown distances and heights based on the channel modeling, making direct distance estimation rather hard [25]. Based on the Lambertian model, in a LoS environment, the received optical power $P_r$ can be expressed as [20]:

$$P_r = \frac{P_t}{d^2} R_o(\alpha) A_{eff}(\theta) T_f(\theta) g(\theta) \tag{2}$$

$P_t$ is the mean transmitted optical power, $d$ is the distance between transmitter and receiver, $\alpha$ and $\theta$ are radiation and incidence angles $T_f$ is the gain of the optical filter and $g$ is the concentrator gain. $R_o(\alpha)$ is the transmitter radiant intensity and $A_{eff}(\theta)$ the effective signal collection area. This approach saves power and time, due to the reduced time of fingerprint matching compared with other approaches, such as triangulation. On the other hand, the pre-calibration of the fingerprints is a mandatory step, as they are affected by the system settings [26].

### B. CHALLENGES IN VLP SYSTEMS

Although VLP methods can provide higher accuracy and performance results for IPSs, than other indoor localization approaches, there are still many open challenges in this field that need to be addressed.

#### 1) MULTI-PATH EFFECTS

The multi-path effect occurs due to the transmitted signals arriving in different paths than the LoS path. The inaccuracies in the received signal can be caused by multi-path reflection on obstacles and walls in the room. These effects greatly impact key parameters such as the RSS, the AoA, and the ToA. Multi-path reflection is higher in the outer areas (corners, edges, etc.) compared to the center of the room. Applying a calibration technique could reduce the percentage error that derives from the multi-path effect [27].

#### 2) INTER-CELL INTERFERENCE

In most VLP systems, there is more than one LED transmitting the location information, at the same frequency band. This may cause signal interference from different LEDs, resulting in a distorted or wrong received signal [20].

#### 3) ORIENTATION OF THE RECEIVER

Most conventional VLP methods require that to determine the receiver's location, its orientation should be known. The majority of proposed solutions assume a constant orientation of the receiver and a certain known height from the ground, resulting in the non-realistic implementation of the VLP systems for real-life situations [20].

While the receiver's orientation challenge is still an area with increased research interest, there have been various research works that try to solve the non-trivial positioning and orientation problem. Authors in [28] propose a novel method to determine both the location and the orientation of the PD array sensors using AoA method. They address the challenge of receiver orientation uncertainty and incorporate it into the ML estimator to improve position and orientation

estimation, achieving an average positioning error of 1.83 cm and an orientation estimation error of 0.04 rad. In [29], the authors develop a novel framework using AoA to locate the tilted receiver, which is either an image sensor or a PD array. Two positioning techniques are studied; one relies on the method of exhaustion (MEX), while the other utilizes the least squares method, without demanding the receivers be placed towards a certain angle, and no additional sensors such as gyroscopes are required. Experimental results indicate that the MEX approach can achieve an average 3D error of 3.20 cm, and the least squares method an average error of 14.66 cm, with the time costs being 0.36 s and 0.001 s respectively. Simultaneous position and orientation estimation is conducted in [30] utilizing RSS values for a VLP system that comprises several LED transmitters and multiple PDs as receivers. Two algorithms are developed, to estimate both the rotation matrix and the location, by leveraging the optimization principle on manifolds to mitigate the constraints imposed by rotation matrix restrictions, thereby enhancing robustness. As proper initialization is required to converge the iterative methods, a coarse estimator employing the direct linear transformation method is suggested. Considering the performance of the estimator as determined by the Cramer-Rao bound, it is deduced that the optimal receiver configuration involves PDs tilted at an angle exceeding 60° relative to the receiver's normal. Shen et al. [31] develop an algorithm for estimating position and orientation in an RSS-based system, employing the hybrid maximum likelihood and maximum a posteriori principle, specifically tailored for a system with multiple LEDs and multiple PD receivers. This algorithm should consider possibly unreliable prior information on the orientation of the receiver. The proposed method closely approximates the theoretical bound when the signal-to-noise ratio (SNR) and the number of LEDs are sufficiently high. Furthermore, it excels in estimating orientation across the entire spectrum of orientation uncertainties due to its effective utilization of prior information, which distinguishes it from other SOTA estimators.

#### 4) NOISE

Noise is a key parameter in any scenario that contains electronic systems. In a VLP use case, the noise can cause major deviations in the position estimation. The noise in a VLP system can be defined as thermal, shot, and dark noise, with the total root mean square noise current magnitude under white Gaussian assumptions expressed as:

$$\sigma_{PD} = \sqrt{\sigma_s^2 + \sigma_{th}^2 + \sigma_{dark}^2} \tag{3}$$

$\sigma_{PD}$ is the noise current magnitude, $\sigma_s$ is the shot/ Poisson noise, $\sigma_{th}$ is the total thermal noise, and $\sigma_{dark}$. Dark noise $\sigma_{dark}$ is created by variations in the PD dark current $I_{PD}$ caused by the thermal excitation of electrons within the silicon chip in the absence of incident photons. The SNR amounts to $I_{PD}^2/\sigma_{PD}^2$ [32], [33]. An effective method to counter the high noise levels is to apply some filtering algorithm, with the most prevalent being, Kalman and particle filter [20].

#### 5) DATABASE CONSTRUCTION

VLP systems can provide high-accuracy positioning services for indoor environments, by exploiting beacon LEDs and PDs. While most of the research on VLP systems has primarily concentrated on pinpointing the location of a PD/PD array target using multiple beacon LEDs with predetermined positions, there are notable challenges in the database construction. The estimated coordinates of LEDs may exhibit fluctuations over time due to environmental factors, as well as the natural aging of the equipment. Furthermore, the process of manually aligning the laser beams with an LED to obtain distance information introduces a degree of inaccuracy in the measurements. This manual alignment process is not only prone to errors but also becomes increasingly burdensome as the number of LEDs in the system grows, necessitating repetitive and time-consuming measurements [34].

To address the database construction challenge, authors in [35] develop a novel system, namely LedMapper, to create precise 3D maps of modulated LEDs in a workspace, efficiently and accurately, with significantly less human effort than traditional manual surveys. This is achieved through the use of a handheld mapping device equipped with visual-inertial sensors, which collects data from the entire workspace. Using the gathered sensor data and reference points, a precise LED map aligned with the workspace is developed. This LED map is designed by formulating a comprehensive simultaneous localization and mapping problem using a factor graph. LedMapper, in contrast to heuristic methods, leveraged input data more effectively due to its well-structured, probabilistic state estimation design. In [34], a beacon LED localization system is introduced for constructing a VLP system's coordinates database. This system utilizes two AOA estimators, each comprising four PDs oriented in different directions to determine the incident light direction. To minimize errors in the LED coordinates database, the AOA estimators should be symmetrically positioned relative to the room center, as demonstrated in simulation results. Theoretical analysis, accounting for thermal and shot noise, predicts centimeter-level accuracy and millisecond-level estimation times in indoor environments.

In [36], a mobile robot serves as a calibration tool for VLP systems. The robot simultaneously performs localization and mapping using a 2D laser scanner to create an environmental map. It also employs a ceiling-facing camera to detect nearby light sources and their frequencies. This combined approach creates an environment map that includes the locations and distinctive identifiers of the light sources. By leveraging the robot's trajectory and the camera's relative position to the robot's center, it becomes possible to translate the motion of each unique light source from the

**TABLE 2.** Comparison of ML approaches of papers.

| *Approach* | *References* |
|---|---|
| ML methods | [6], [8], [11], [16], [37]–[63] |
| RL methods | [64]–[66] |
| DL methods | [9], [25], [51], [53], [57], [62], [67]–[90] |
| EAs | [91]–[118] |

image frame to the map frame. This approach allows for accurate estimation of light source modulation frequencies, enabling their unique identification. Moreover, the inter-LED distances are determined with an average accuracy of less than 10 cm compared to the actual distances, yielding a highly precise automated calibration system.

#### 6) MINIMIZE CALCULATION TIME

Estimating the position of the receiver can be rather complex and time-consuming as certain procedures are needed, such as data collection, applying positioning algorithms, and optimizing them to reduce positioning errors. So, designing a system model, which can offer real-time positioning and navigation services poses a significant challenge when more than one LED is transmitting the location information.

## IV. RESULTS AND DISCUSSION

This section provides the findings and statistics extracted from the research methodology described in Section II. Also, a brief presentation of the AI methodologies, along with a detailed discussion of the ML and evolutionary algorithms (EAs) in the included papers, is conducted.

### A. PAPER STATISTICS

The majority (60/88) of the research papers that are included in this methodological review use ML approaches to enhance the accuracy and performance of VLP systems, whereas the rest 28/88 utilize evolutionary methods to optimize the position estimation in VLC systems. The ML approaches can be distinguished into three major categories: ML, deep learning (DL), and reinforcement learning (RL) methodologies. 27/60 of the papers use ML approaches, 26/60 utilize DL methods, whereas RL is applied only in 3/60 of the reviewed papers. Finally, in 4/60 of the included papers both ML and DL methodologies are combined to estimate the position and location of the receiver in VLC systems. 49/88 studies are conducted for 2D estimation of the receiver's position and the rest (39/88) estimate the 3D position of the PD receiver. Also, 52/88 conduct an experimental study in the estimation, whereas 36/88 of the papers describe simulated environments and results. The paper statistics are shown in Table 2, Table 3, and Table 4 for each of the above described category.

**TABLE 3.** Comparison of estimation environment in papers.

| *Estimation environment* | *References* |
|---|---|
| 2D | [6], [8], [9], [16], [37], [38], [40]–[43], [45]–[59], [61], [64], [66]–[68], [70], [72], [73], [75]–[77], [79], [84]–[86], [88]–[90], [101], [102], [107], [108], [114], [115] |
| 3D | [11], [25], [39], [44], [60], [62], [63], [65], [69], [71], [74], [78], [80]–[83], [87], [91]–[100], [103]–[106], [109]–[113], [116]–[118] |

**TABLE 4.** Simulation/experiment-based taxonomy in included papers.

| *Simulation/experiment* | *References* |
|---|---|
| Simulation | [9], [39], [42], [43], [47], [48], [52], [60], [62], [67], [69], [70], [72], [74], [77], [83], [84], [88], [91], [92], [94]–[96], [99], [100], [103]–[105], [107], [109]–[115] |
| Experiment | [6], [8], [11], [16], [25], [37], [38], [40], [41], [44]–[46], [49]–[51], [53]–[59], [61], [63]–[66], [68], [71], [73], [75], [76], [78]–[82], [85]–[87], [89], [90], [93], [97], [98], [101], [102], [106], [108], [116]–[118] |

### B. AI METHODOLOGIES

AI and ML offer promising avenues to enhance the intelligence of communication nodes. This makes them valuable for tackling intricate challenges that often demand extensive iterations with conventional methods or scenarios without straightforward solutions. In the realm of wireless communication, ML has evolved to a level where it empowers wireless systems to engage in data-driven interactions for understanding and extracting information [119]. Through these data-driver interactions, AI can offer various solutions to the challenges of IoT networks, which employ a massive amount of data generated from smart devices. ML algorithms possess a key characteristic: they don't require prior knowledge of the physical model; instead, this information is ingrained within the training set. For instance, in scenarios relying on RSS, precise details such as the receiver or transmitter orientation and radiation pattern angles are vital for accurate localization through analytical methods. In addition, traditional physical models struggle with issues like noise, unfamiliar radiation patterns, obstructed views, and dust. Data-driven approaches can offer solutions to address these problems and challenges [6]. In VLP systems, environmental factors significantly impact performance; for example, inter-cell interference can make RSS data inaccurate, leading to positioning errors. AI can enhance accuracy and simplify calculations for VLP systems by considering inter-cell interference during training, thereby sidestepping complex model computations [59], [82].

AI methods can utilize these data to provide accurate and robust indoor services, including localization, position estimation, optimal resource allocation, and activity recognition [120].

The high-precision positioning problem in VLC systems can be addressed as a multi-parameter optimization problem, while ML and evolutionary methods can offer robust and accurate results.

#### 1) ML

ML is a subclass of AI that involves learning discriminative features about a system using computational methods. These approaches utilize available data and information to make accurate predictions in tasks such as classification, regression, and interactions between an intelligent agent and an environment [121]. Recently, ML has been widely applied in wireless communication scenarios. ML is a data-driven approach, providing accurate and robust results regarding the positioning accuracy of the receiver. Also, there is no need to quantify every parameter of the VLP model or describe the underlying physical model, thus reducing the complexity [6]. Deep learning (DL) is a highly promising sub-field of ML that has facilitated the development of numerous advanced technologies. DL algorithms have the ability to learn automatically from basic to intricate features as they progress from shallow to deeper layers of artificial neurons, using the stochastic gradient descent algorithm to train the model. DL models pose as accurate and robust approaches in various fields and applications [122]. ML can be distinguished into three main techniques: supervised learning (SL), unsupervised learning (UL), and reinforcement learning (RL).

- Supervised learning: SL includes learning models that are built based on labeled data. The data include known input features or independent variables $\mathbf{x} = (x_1, x_2, \ldots x_n)$ and a known output target or dependent variable $y$. SL models try to predict the function $h$ such as $y = h(\mathbf{x})$, through the learning process. The process stops when the estimation performance of the model is considered satisfactory, and then the trained model can determine an unknown output target, given new values of input features. Mathematically, the SL process may be formulated as follows: Given a set of M examples $(x_i, y_i)$ and defining a proper loss function $\mathscr{L} : Y \times Y \rightarrow \mathbb{R}^d$, the goal is to minimize the objective function

$$\mathscr{C} = \frac{1}{M} \sum_{i=1}^{M} \mathscr{L}(y_i, h(x_i)) \tag{4}$$

  SL algorithms can be used for both regression and classification problems. In regression tasks, the estimated output $y$ of the model is a continuous variable, whereas, in classification problems, discrete values are considered [123]. Commonly used SL techniques include linear regression (LR), ridge regression (RR), Gaussian process (GP), k-nearest neighbors (kNN), support vector machine (SVM), and decision trees (DTs). Also, fully connected feed-forward neural networks (FNNs), convolutional neural networks (CNNs), recurrent neural networks (RNNs), artificial neural networks (ANNs), and long short-term memory (LSTM) networks can be regarded as supervised algorithms [121].
- Unsupervised learning: ML algorithms that utilize unlabeled input data $x$ to extract and learn patterns for the unknown output target $y$ can be categorized as unsupervised. UL approaches group data into clusters based on the similarities between the data samples. The samples that are closest to a defined center cluster are grouped in the same cluster and the process is repeated. The clustering procedure ends when the function

$$g = arg \min \mathscr{D} \tag{5}$$

  is minimized. $\mathscr{D}$ is the distance metric, with Euclidean, Manhattan, Minkowski, and cosine index distance being widely used [123]. Some typical UL methods include k-mean clustering, density-based spatial clustering of applications with noise (DBSCAN), as well as autoencoders (AEs) [121].
- Reinforcement learning: RL is an algorithmic process in which an intelligent agent learns based on a sequence of interactions enabled by a feedback loop with the environment. The agent updates its state and selects the next action by trial and error, based on whether the taken action resulted in a reward or penalty. The objectives of the agent are defined based on the maximization of the rewards over a set of actions with the interacting environment to learn the best policy [123]. RL algorithms can be distinguished into value-based (Q-learning) and policy-based algorithms (policy gradient (PG), actor-critic (AC)) [124].

#### 2) EVOLUTIONARY ALGORITHMS

EAs have been demonstrated as effective tools for parameter optimization and are widely used to tackle various challenges in wireless systems in an acceptable computational time [125]. In this work, only EAs that belong to AI methodologies are considered. This class of EAs is inspired by the organized collective behavior of social insects/animals, biological evolution, and the rules that govern natural phenomena. Based on these inspiration mechanisms, EAs can be distinguished into three categories: swarm intelligence algorithms (SIAs), genetic programming (GPR), and differential evolution (DE)-based algorithms respectively [126], [127]. To overcome the recent challenges in indoor positioning applications, research utilizes evolutionary approaches to enhance the performance of localization estimation in VLP systems. The EAs taxonomy along with the most commonly used EAs in VLP systems is depicted in Fig. 7. The ML and evolutionary methods will be analyzed in Section IV-C.

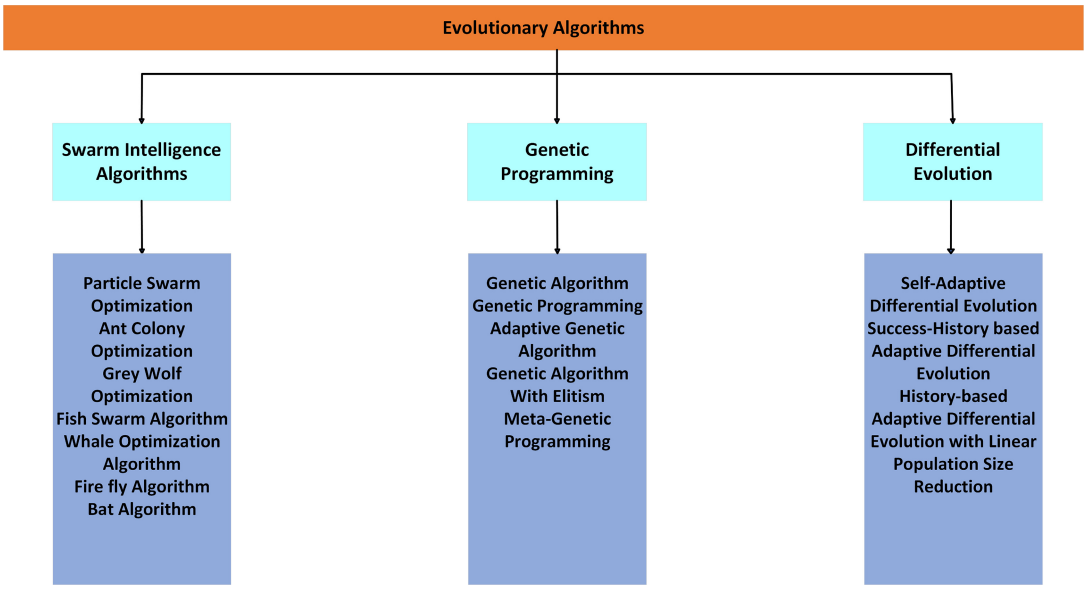


**FIGURE 7.** Evolutionary algorithms taxonomy.

### C. DISCUSSION

In this review, ML and meta-heuristic approaches for positioning in VLC systems are analyzed to determine the impact and possible enhancement of robustness and performance. This study aims to provide a detailed analysis of the AI methodologies, techniques, and algorithms utilized in VLP systems for indoor IoT applications.

#### 1) ML METHODS

Among the included research papers, ML is the most widely used. Various conventional ML methods are utilized in VLP systems, including kNN, k-means, DBSCAN, LR, DTs, RR, GPs, support vector regressor (SVR), and extreme learning machines (ELMs).

The classic kNN algorithm is one of the most fundamental and simple supervised ML algorithms. It is a non-parametric method utilizing a local approximation, which is mostly used for classification problems but also performs well with a small amount of data in regression problems. In the regression problem, the estimated values are taken as the mean value of its k nearest neighbors. KNN might be efficient and robust, but it also presents various drawbacks: it is a distance-based approach, the central core of the kNN is distance-dependent, and its simple Euclidean distance metric is not suitable for high-dimensional data. Variations of the kNN approach have been developed to address these challenges, with weighted kNN (wkNN) being widely used in VLP scenarios. wkNN is a robust extension of the kNN method that uses the distance between neighbors, calculating the mean of the k nearest data points as the estimation output [128].

The authors in [40] apply a wkNN to estimate the 2D position of a PD receiver, using the RSS fingerprinting technique. To enhance the accuracy of the wkNN, fabricated RSS data are generated based on the Lambertian optical propagation model, to create a dense fingerprint map. The square chord distance produces the best localization accuracy of 2.7 cm, using only a small number of off-line measurements, and the wKNN model can easily be trained and calibrated. The work presented in [52] is a combination of optimal kNN (okNN) and wkNN, namely weighted optimum kNN (WokNN), to estimate the 2D location of a PD receiver based on RSS measurements.

OkNN automatically determines the optimal number of k-nearest neighbors for each position, and wkNN is utilized to minimize the possible error from averaging the Euclidean distance in each position. As this process is computationally expensive, a maximum received signal strength recognition (MRR) technique is applied to decrease the computational cost. The implemented approach achieves a very low mean positioning error of 0.8 cm, while the computational time is reduced, through the MRR, by $42\% - 52\%$ for each area of interest. Reference [54] proposes a novel wkNN, namely Watchers on the Wall, to estimate the 2D location of a mobile target, based on the deviations in the RSS measurements recorded on a wall-integrated light sensor array. The weights of the model are computed based on the Manhattan or Canberra distance and the mean positioning accuracy of the approach is 12 cm for a mobile receiver along multiple routes. While the proposed method may produce precise results, it requires significant computation time, since creating the fingerprint database is an extremely time-consuming procedure.

In [16] a wkNN approach is studied that estimates the 2D location of a PD receiver, utilizing sparse fingerprints. The model is trained to utilize an artificial dataset that is constructed based on a modified path-loss model. The path-loss exponent is considered to be variable and the optimum path-loss exponent calibration is achieved via bicubic interpolation. The wkNN approach can achieve an average positioning accuracy

of 1.92 cm when utilizing fabricated RSS fingerprints. Abu Bakar et al. [55] present a wkNN model for the 2D localization of a custom-made tag PD receiver. A dense RSS fingerprint dataset is constructed to reduce computation time, and the Manhattan distance metric provided better accuracy results than the Euclidean and Matusita distance metrics. The wkNN approach achieves a median positioning error of 4.62 mm when using four luminaires, and 9.87 mm can be achieved with two luminaires.

In [49] a novel positioning method, based on weight coefficients k-nearest neighbor (WCkNN) and multitask learning (MTL), is utilized to estimate the 2D location of a PD receiver, employing Wi-Fi, Bluetooth, and magnetic field fingerprints. The MTL fuses and finds the correlation between the features of the fingerprints, whereas the WCkNN estimates another location in a certain class based on the obtained position. The receiver's position is estimated by combining the projected locations, via a weight-averaging procedure, where the weights correspond to the positioning errors, obtaining an average positioning error of 195 cm. DNN-based positioning error prediction models generate positioning errors by computing the discrepancies between each projected position coordinate and the actual position coordinate. Tran and Ha in [42] combine kNN and random forest (RaF) to estimate the 2D coordinates of a PD receiver, under the effect of multipath reflections. kNN expands the number of RSS features, and the most prominent are utilized as inputs to the RaF to reduce the complexity and computation cost. The proposed method achieves an average positioning accuracy of 2 cm, five times better than other popular kNN approaches. The authors achieve exceptional positioning accuracy beyond the center of the room, where the highest multipath reflections occur, taking into account factors such as ambient light, thermal noise, and shot noise, in addition to the highest reflection rate.

RaF is an ensemble learning technique that combines various DTs. Each DT in the model is trained and constructed consequently without being pruned on a bootstrap training set, and the excluded (in the training) samples are called out-of-bag. The DT chooses the split with which the highest homogeneity is acquired, while the candidate features for each split are randomly selected. If there can be no split (i.e., maximum depth or minimum leaf size is reached), then the node (leaf) is regarded as terminal. The number of possible features of each split greatly impacts the diversity of the DT and low bias can be acquired based on the minimum terminal leaf size, thus controlling the complexity of the approach. The robustness and stability of the RaF method are greatly affected by the number of DTs included. The predictions are more stable and robust, as the forest is expanding. RaF is a very popular ML approach in regression problems because it can acquire great performance and avoid overfitting in a wide spectrum of applications [129].

In [41] authors propose a DT model, an enhanced J48 tree algorithm, to estimate the 3D indoor and underwater location of a PD receiver, by using RSS samples. The estimation is based on optical signal information received at the PD, which is converted into an electrical signal, to reach a microcontroller, directing the information to the receiver computer. The model is trained in a simulated underwater environment and tested in a 3D simulation room, thus is viable for both air and underwater systems, obtaining an average positioning error of 11 cm. Authors in [62] various ML methods (i.e., DT, SVM, and NNs) are presented and compared for 3D indoor localization of PD receiver, based on RSS fingerprints and the angles of a steerable laser. All the ML models acquire the RSS values, angles of the laser, and the related position through predetermined reference points to determine the receiver's position. Using the laser's angles as inputs to the ML models reduces the localization error, with the DT outperforming the rest, with an average positioning accuracy of 3.8 cm.

The k-means algorithm is one of the most popular unsupervised learning methods applied to the well-known clustering problem. Assume a dataset $A = [a_1, a_2, \ldots, a_n]$ in a d-dimensional space and $C = [c_1, c_2, \ldots, c_n]$ the m centers of the cluster. Let $y = |y_{ik}|_{nxc}$ with $y_{i_k}$ a binary variable that determines whether each sample $a_i$ is within a k-th cluster, $k = 1, \ldots, m$. The Euclidean distance between each data sample $a_i$ and cluster center $c_l$ can be defined as $r = ||a_i - c_k||^2$. The k-means algorithm iterates and tries to minimize the objective function $F(y, C) = \sum_{j=1}^{n} \sum_{i=k}^{m} r y_{i_j}$ while updating the cluster centers and data points in each iteration. The major drawback in real k-means clustering approaches is to give an unknown number of clusters a priori. Moreover, each initialization and iteration greatly impact the algorithm [130].

In [46] a k-means clustering method is applied to estimate the 2D position of a PD receiver, with an average positioning accuracy of 31 cm and a standard deviation of 21 cm. The RSS values are calculated at the receiver end, and a sparse grid is defined based on the light intensity at different location points. The ML model is trained based on a dense grid of readings, by utilizing a bilinear interpolation, and offers accurate localization results based on only two transmitters. k-means clustering in conjunction with linear regression is applied in [39], to estimate the 3D position of a PD receiver. The experimental setup consists of RSS values from multiple LED transmitters that formulate a cube, generating a fingerprint map. The positioning accuracy of the regression approach on the clustered data is significantly improved from 70 cm to 40 cm in the 3D environment. A fusion of k-means clustering and RaF is applied in [44] to determine the 3D coordinates of a PD sensor, based on RSS values. The clustering method enhances the positioning accuracy by dividing the RSS dataset into k groups with high similarity, and the RaF approach achieves a positioning accuracy of 10 cm, as it is less susceptible to multi-path propagation compared with other methods. In addition, as the RaF conducts the location estimation in each data cluster, the execution time of the estimation process can be significantly reduced.

DBSCAN is one of the most important density-based clustering algorithms. It can identify outliers and cluster arbitrary shape distribution in the data. It depends on two parameters, the scanning radius and the density threshold, to define whether a data point is regarded as a core point or not. DBSCAN has strong adaptability, but is used mainly for high-dimension data points, as it suffers from the curse of dimensionality [131].

In [60] authors develop a hybrid algorithm based on the ELM and the DBSCAN to estimate the 2D position of a PD target, using only a single LED. The PD is rotatable and measures the angles in relation to the LED projection point together with the RSS values. First, the RaF method is applied to classify two parts in the area of interest; the corners zone and the interior zone. For the latter, the horizontal distance from the PD and angles can be utilized to infer position. For the corner zone, the hybrid approach is applied, where the ELM roughly estimates the position of the target, and as the rotatable PD is moved the coordinates are re-estimated. DBSCAN finds the largest cluster and its weight corresponding to the location of the target, enhancing the mean positioning accuracy at 1.74 cm. The authors in [47] propose a DBSCAN approach combined with an outlier removal strategy to estimate the 2D coordinates of a positioning sensor, consisting of several PDs placed into a predetermined number of meridians and parallels in a hemispherical area. Three emitter combinations are utilized to generate position estimates for the outlier removal, which are then filtered using the DBSCAN method and fine-tuned using LR. The suggested method improves positioning precision, by a mean 35% of than conventional trilateration, with an average positioning error of 3.5 cm, but with a moderate increase in algorithm complexity.

LR aims to find the correlation between an independent variable $x$ and the dependent variable $y$. The equation describing the linear regression is $\boldsymbol{y} = a\boldsymbol{x} + b$, where a is the slope of a regression line and b is the intercept. If $a > 0$ the correlation between the variables is considered positive and if $a < 0$, negative. If $a = 0$, there is no correlation between $X$ and $Y$ variables [132].

To reduce the data collection workload, the authors in [56] apply LR in a simulated and experimental use case scenario to design an indoor VLP system, and accurately estimate the 2D location of a PD receiver. The DIALux software is utilized to formulate the simulation environment, obtaining results close to the experimental setup, with the mean positioning error of 11.1 cm and 10.5 cm, respectively. By utilizing the least square method in the model, it becomes non-iterative, which diminishes both training time and complexity. The results indicate that DIALux can generate suitable data when the room's size and the LED luminary's specifications are known, thereby easing the task of collecting training data in VLP systems.

RR is an ML technique that introduces a hyper-parameter in multiple LR methods, to achieve optimization through the regularization of data. RR attempts to minimize the sum of squared residuals by finding a linear function, represented by $f(x) = \sum_{i=1}^{n} x_i w_i$, that best fits a dataset of N points $(\boldsymbol{x_i}, y_i)$ using the fitting parameters $\boldsymbol{w} = (w_1, .., w_N)$. In order to accomplish this, RR employs a regularization factor that helps to minimize the distance between $f(x_i)$ and $y_i$ while simultaneously minimizing the sum of squared residuals for the $\boldsymbol{w}$ parameters:

$$\boldsymbol{w} = \underset{\boldsymbol{w}}{arg\,min} \sum_{i=1}^{n} |f(\boldsymbol{x_i} - y_i)|^2 + a|\boldsymbol{w}|^2 \tag{6}$$

The data samples are clustered along the same center, while the subspace is considered to be null [133].

The authors in [50] demonstrate an AoA-based VLP localization system based on third-order RR and quadrant-solar-cells (QSCs). The RR is utilized to obtain the weight vector $\boldsymbol{w}$, thus greatly enhancing the accuracy of the AoA method, as the average positioning error is reduced from 7.2 cm to 3 cm, showing an improvement of 57% in terms of positioning accuracy, for the camera-based receiver. In [11] a sigmoid function data preprocessing method is applied to LR and RR models, to estimate the 2D location of a PD target. The RR outperforms the LR with a mean positioning error of 2.06 cm and greatly improves the positioning accuracy by a mean of 42.6% for the horizontal and vertical axes.

GP is a popular nonparametric ML approach in various regression applications, in which the regression form is specified by a mean vector $\boldsymbol{a}$ and a covariance matrix $\boldsymbol{R}$. Let $(x_i, y_i)$ be a given dataset of m points and a Gaussian distribution $\mathcal{N}((\boldsymbol{a}, \boldsymbol{T})$, then the target values can be expressed as:

$$y(x_n) \sim \mathcal{N}(m(x_n), \sigma^2) \tag{7}$$

where $m(x_n)$ is the mean measurement for a point $x_n$ and $\sigma^2$ corresponds to the noise variance. The mean measurement $m(\boldsymbol{x}_n)$ can be expressed by the Gaussian distribution $m(\boldsymbol{x}) \sim \mathcal{N}(0, k_\phi)$, with $k_\phi$ parameterized by the $\phi$ kernel for the measurements [134].

SVR is a robust end-effective supervised extension of SVMs when dealing with regression problems. Considering a dataset of $m$ inputs and corresponding target values $x_i, y_i$ and the implicit function $g$, the SVR methods try to minimize the $\epsilon$-insensitive loss function $L$:

$$L(y, f(\boldsymbol{x}, \boldsymbol{g})) = \begin{cases} 0, & |y - f(\boldsymbol{x}, \boldsymbol{g})| < \epsilon \\ |y - f(\boldsymbol{x}, \boldsymbol{g})| - \epsilon, & \text{otherwise} \end{cases} \tag{8}$$

Unless the kernel function $f(x)$ is linear, the training data will be transformed into a high-dimensional space by means of the function $g$. There are some drawbacks in the SVR approach, such as difficulty in parameter tuning and choosing the proper kernel function, and the large computation time needed for large datasets [135].

Knudde et al. in [6] present and compare two ML methods (i.e., MLP and GP) with a conventional multilateration approach for 2D position estimation of a PD receiver, when there is a random transmitter tilt. Both ML algorithms greatly outperform the conventional approach, while GP achieves

an average positioning accuracy of 2.45 cm against 2.8 cm of the MLP, thus being very practical and accurate when the available training data are limited. GP and MLP are also compared in [51], using relative RSS input features. Various datasets were utilized, modifying per dataset either the LEDs power or the aperture of the PD receiver. The ML models are compared to a conventional multilateration approach for two schemes, one where the RSS vector is normalized using the maximum received light intensity, and the other where the RSS vector is formulated by merging the received intensities. The ML models outperform the conventional multilateration method in all use-case scenarios and datasets. GP also achieves better average positioning accuracy than the MLP for both RSS schemes; in more detail, the $p_{95}$ error obtained in the two scenarios is 7.19 cm, 7.72 cm, and 7.17 cm, 7.55 cm respectively.

In [8] the measured intensity values are used to predict the 2D position of a mobile PD receiver through a GP model. A new active learning (AL) method is utilized to extract the most important receiver locations, based on the maximum variation in the RSS values, thus accelerating the data collection process. Then, an inverse GP is applied to estimate the position of the PD, based on the previously collected data. The AL strategy prevents instabilities/deviations in the final GP prediction model, which is enhanced by measuring RSS values at positions forming a straight line with the locations obtained from the AL methodology. This approach outperforms maximum variance sampling and random sampling methods, obtaining an average positioning error below 10 cm. Aparicio-Esteve et al. in [59] compare a conventional triangulation algorithm based on AoA with a GP for 2D visible light positioning estimation. Both approaches utilize RSS values on the quadrant PD receiver with an aperture, to acquire the image points from each transmitter on the PD, and, through a least squares estimator (LSE) and trigonometry, predict the location of the PD. An AE is employed in the initial step of the data-driven method to reduce the input dimensionality and produce features that will be utilized as inputs for the GP, which then produces more accurate position estimates. The GP outperforms the triangulation algorithm, as the $p_{95}$ error is 16.65 cm and 21.94 for the entire area, respectively. In addition, GP can offer robust estimation results in the corner of the experimental setup, as the $p_{95}$ error is 10.35 cm, while for the triangulation approach 18.56 cm.

ELMs have demonstrated their effectiveness and robustness in ML for a wide range of applications, including classification and regression problems. Developed for FNNs, ELMs have garnered attention due to their rapid learning speed and excellent performance in various use cases. The ELM was first developed for a single hidden layer FNN and given a training data set $\{\boldsymbol{x_i}, y_i\}_i^N$ can be expressed using matrix multiplication:

$$\boldsymbol{Hw^o} = \boldsymbol{O} \tag{9}$$

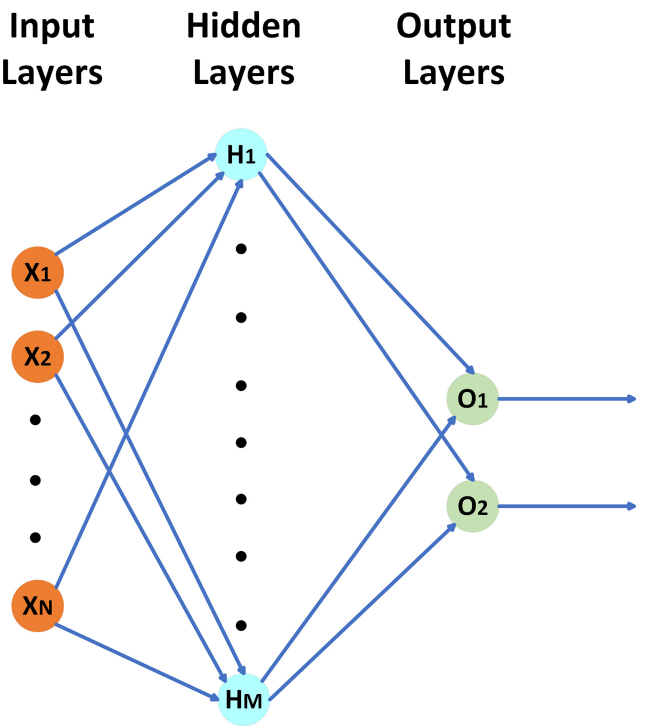


FIGURE 8. MLP architecture.

$\boldsymbol{H}$ is the hidden layer output matrix, $\boldsymbol{w} = [\boldsymbol{w_1}, \boldsymbol{w_2}, \ldots, \boldsymbol{w_L}]$ the input layer weight matrix, and $\boldsymbol{O} = [\boldsymbol{O_1}, \boldsymbol{O_2}, \ldots, \boldsymbol{O_N}]$ the output matrix of the model. $\boldsymbol{H}$ can be expressed as a matrix $G$ as follows:

$$\boldsymbol{H} = G(\boldsymbol{V}) \tag{10}$$

$V$ is the matrix of hidden layer inputs for all the given training samples and is defined as:

$$\boldsymbol{V} = \begin{bmatrix} w_1 x_1 + b_1 & \cdots & w_L x_1 + b_L \\ \vdots & \cdots & \vdots \\ w_1 x_N + b_1 & \cdots & w_L x_N + b_L \end{bmatrix}_{LxN} \tag{11}$$

$\boldsymbol{b} = [\boldsymbol{b_1}, \boldsymbol{b_2}, \ldots, \boldsymbol{b_L}]$ is the output layer weight matrix Based on (11) the ELM focuses on minimizing the training error of the process $err$, which can be expressed as

$$err = \min_{\boldsymbol{b}} ||\boldsymbol{Hb} - \boldsymbol{T}||_F^2 \tag{12}$$

with $\boldsymbol{T}$ the matrix of the output targets and $||\cdot||_F$, the error matrix normalization (i.e., Frobenius matrix) [136].

In [63] a VLP system that uses fingerprinting and the ELM algorithm is presented for real-time 3D positioning, assuming that the PD receiver is perpendicular to the ceiling and has no tilt. The indoor positioning environment is first split into conventional VLP kernels to reduce the fingerprint database's size and corresponding training time. The implemented method is resistant to noise interference and can achieve accurate real-time 3D positioning, with an average positioning accuracy of 3 cm.

In [37] grid-dependent least squares (GD-LS) are utilized to improve the accuracy of a localization method that

combines several classifiers based on RSS values. In this approach, different intensity-modulated sinusoidal signals from LEDs are recorded by PD receivers positioned at different grid points. The GD-LS method exhibits numerical stability when dealing with singular output matrices and is robust to the inaccuracy of RSS values. In contrast to trilateration strategies, GD-LS does not rely on the model parameters and no prior knowledge of the position of the LEDs is required, is more robust to model errors, and achieves an average 2D positioning accuracy of 5 cm. Tran and Ha in [58] develop a novel algorithm, namely Ada-XCoReg, that combines the improved co-training semi-supervised regression and adaptive boosting approaches, to reduce the burden of data collection and enhance 2D positioning performance of a PD target. The improved co-training supervised regression (XCoReg) determines the positions of unlabeled data and removes unnecessary data, based on a wkNN method and cross-correlation techniques. Then, adaptive boosting is applied to enhance the performance of the previously labeled data, achieving a positioning accuracy of 2.51 cm.

In [45], a two-layer fusion network (TLFN) indoor localization approach, made up of the diverse and the fusion layer, is proposed. TLFN is a VLP system that utilizes multiple combinations of fingerprints and classifiers to obtain several position estimations in different layers.TLFN minimizes the average localization errors for all fingerprints and classifier spaces and saves weights for each grid point in the fusion layer, to estimate the 2D position of a PD receiver based on the RSS values. During the online phase, an optimal weights search strategy is utilized to perform the fusion localization. A higher and more stable average positioning accuracy of 5 cm can be achieved, as the TLFN leverages the intrinsic supplementation among multiple position estimates. The authors in [43] study a signal pre-processing technique combined dual-function ML algorithms, performing classification and regression procedures. The pre-processing involves removing low-intensity reflected signals and noise filtering. The classification and sequential regression process included a comparative study of four methods, namely SVM, DT, RaF, and kNN. SVM outperformed the other approaches, with the classification function reducing the execution time by 78%, while the regression function helped determine the PD receiver location with an average 2D positioning accuracy of 8.6 cm.

A second-order regression method is studied in [48] to improve 2D positioning estimation accuracy in a VLP system that uses repeated cell strategy. The maximum likelihood and least squares are used to obtain the model weight vector, and the PD receiver cell position can be obtained by utilizing the target vector of the training process to replace the amplitude vector of the approach. The proposed method achieves a mean positioning accuracy of 4 cm, outperforming conventional RSS-based localization methods, at the cost of higher complexity. In [61] a generalized Gaussian distribution (GGD) approach is designed, which scores a 98% classification accuracy for the position area of the mobile node receiver, with limited NLoS training data for an ultra-wideband (UWB) IPS. For the GGD, the LoS and NLoS signal features are extracted, and the distribution of each feature is utilized to build the model.

### 2) DL METHODS

DL methods are accurate and robust approaches for position estimation in the included VLC systems. Several NNs architectures (e.g., CNNs, ANNs, RNNs), as well as adversarial deep learning, are applied in the included works.

Artificial neurons (ANs), are the fundamental units of DL architectures and are inspired by the structure and function of biological neurons in the human brain. ANNs are comprised of multiple ANs layers. The ANN architecture is formed by using input, hidden, and output layers, utilizing various training methods, such as error backpropagation and biologically plausible techniques. The hidden layers are used to process the input data and compute the model's prediction to be sent to the output layer. Recent research advancement in IoT applications has significantly increased the need for accurate information and feature extraction and ANNs pose as an important tool in this manner [137].

The authors in [70] propose a convolutional stacked auto-encoder (CSAE) to exploit the spatial and temporal interdependence present in RSS temporal image (RTI) data, which consists of a sequence of successive RSS measurements as input. After the CSAE extracts and learns the stable and latent features from the data, a regression ANN method is utilized to acquire more intricate and consistent characteristics from the varying RSS readings and achieve improved 2D position estimation. The proposed method obtains more accurate and consistent positioning results from fluctuating RSS data compared to conventional ANN techniques, as the fluctuating noise is reduced, leading to an average positioning accuracy of 32 cm. A three-layer ANN is applied in [67] to accurately predict the 2D coordinates of a PD location point in an indoor environment. TDOA at the receiver point from different LEDs is utilized to construct the data feature, in order to perform feature extraction. These extracted features are introduced as input in the ANN model, achieving an average positioning error of 1.66 cm. The proposed model presents improved robustness by ensuring the mapping relationship between delay estimation and coordinates. In [71] a 3D positioning system is employed, which uses an ANN model consisting of nine input layers, two hidden layers, and three output nodes. RSS values that formulate a grid, are introduced as inputs to the ANN, achieving an average positioning error of 0.9 cm, which is much lower compared to the dimensions of the mobile PD receiver.

An ANN architecture is utilized in [25] to address the complex trilateration approach for a 3D VLP system, comprising of LED transmitters and a PD receiver. Compared to conventional trilateration methods, the ANN-assisted trilateration approach can provide an accuracy of 11.93 cm

with a computation time that is 50 times faster. The trilateration problem is simplified by representing it as a linear mapping, which greatly reduces its complexity and leads to faster position estimation, resulting in a significant reduction in computation time. A hybrid single hidden layer ANN is applied in [74] with pre-training techniques to enhance the robustness of a PD receiver positioning method. The proposed hybrid system has an accuracy of 1 cm and also high adaptability, robustness, and lower complexity in offline and on-line deployments, compared to conventional methods. Ni et al. in [75] present a single hidden layer ANN for the experimental 2D position estimation of a PD receiver, utilizing LED signal with two frequency response matrices, obtained with Alamouti space-time block coding (STBC) to mitigate the effects of different transmission path lengths in this multiple-inputs and single-output (MISO) system. The average positioning error of the ANN is 0.73 cm, offering simultaneous indoor visible light communication and positioning services.

The authors in [82] propose an innovative method for correcting deviations, namely memory-artificial neural network (M-ANN) to accurately predict the 3D coordinates of a PD receiver, based on the RSS values from the LEDs. In this model, a memory module is added to a two-layer ANN to create a cell, obtain features as a sequence of discrete test moments, and prevent large errors in case of emergencies. This model, utilizing a GA module, can replace missing RSS values, due to possible blocked LEDs, offering an accuracy of 3.53 cm in the worst-case scenario of 2 blocked LEDs. In [88] various ANNs are employed for the 2D localization of a PD sensor receiver, considering a multi-path channel. The ANN with Bayesian regularization can outperform conventional RSS techniques, utilizing non-linear least square estimation for the SNR values, with the mean positioning error being 2 cm for 30 dB of SNR.

Majeed and Hranilovic in [84] implement an ANN for passive indoor visible light 2D position estimation, utilizing RSS fingerprints to predict the PD receiver location. The proposed ANN does not require active participation from the user and learns the correlation between impulse responses and receiver positions, achieving an average positioning error of 80 cm with a limited training data set and without the need for active user participation. In [81] an ANN is utilized for a conventional VLP monitoring system, consisting of a single LED as the transmitter and a standard surveillance camera as the receiver. The ANN can offer an accurate 3D position estimation, even when the target is inclined at different angles, with a mean positioning error of 0.65 cm and 0.67 cm for 15° and −15°, respectively. The authors in [53] propose a VLP scheme utilizing silicon photovoltaic cells and ANN for 2D position estimation based on AoA and RSS methods. This approach can offer a positioning accuracy of 2.99 cm and 2.60 cm for AoA- and RSS-based systems. Zhang et al. in [73] a Bayesian regularization deep neural network (BR-DNN) exploits sparse RSS values and BP and is trained using the Levenberg-Marquardt algorithm, to estimate the 2D position of a PD target. The weights and bias are updated by Bayesian regularization and are tested in three distinct layout configurations, namely the even, arbitrary, and diagonal sets, with the average positioning error under the diagonal set being 3.4 cm, while maintaining a high convergence rate lower than 9 ms.

In [68] a FNN is utilized to extract features and obtain the relative distance between a camera-based receiver and the transmitting LEDs, considering that the tilt and angle of the receiver to be fixed and known. The 2D position coordinated with the receiver is then estimated based on the triangulation algorithm and the mapping of the relative distance performed from the MPL, achieving a mean positioning error of 1.9$cm$. Alonso-González et al. in [69] propose an RSS fingerprinting indoor 3D positioning estimation based on FNN to estimate the location of a mobile PD receiver. In the system under study, the positioning problem is broken down into three FNN models, one per axis. An array of RSS values is utilized as inputs to each model, taking into account multi-path reflections and random orientation angles for the receivers. By optimizing the nodes of each layer for each model, the proposed method achieved a positioning accuracy of 1.9 cm for the 3D environment. In [79] two FNN approaches are considered for 2D position estimation of a PD target, in a large industrial experimental environment with several large machines of obstacles. Two approaches are studied, an FNN covering the entire and a cellular approach in which a less complex FNN is applied per allocated cell. For the latter approach, a kNN classification of the positioning cell is required to accurately infer location estimations. Both approaches can offer accurate position estimations, below 10 cm, with the cellular approach having a mean positioning error of 4.2 cm versus 4.3 cm of the single FNN approach. The single FNN approach might be more straightforward in terms of hyper-parameter tuning, but the cellular approach is more accurate, improves scalability, and lessens the chance of overfitting. The authors in [78] apply a supervised feedforward BP FNN model to provide an accurate 3D estimate for the location of a PD sensor, utilizing RSS fingerprints. In this study, multi-path propagation is considered, and utilizing receiver diversity (i.e., placing the receiver in different positions) significantly enhances the 3D position estimation, for both LoS and nLoS scenarios, with average positioning errors of 1.98 cm and 2.10 cm respectively.

CNNs are a class of ANNs that utilize convolution operations instead of matrix multiplication, to learn the feature representation of data. The core structure of a CNN consists of the input layer, the convolution layers, the pooling layers, and the output layer [138]:

- Input Layer: In this layer, the input data are introduced in a suitable format for further processing, to extract high-level features through a series of hidden layers.
- Convolution Layers: In this section, the convolution of data parameters is computed through multiple filters of equal shape with the input layer, but smaller dimensions.

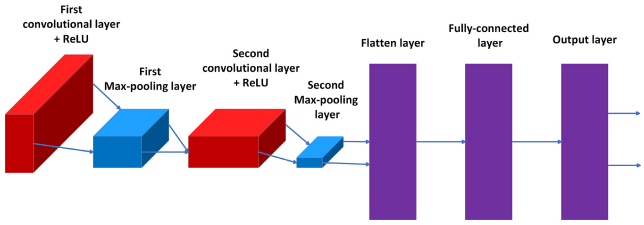


**FIGURE 9.** CNN architecture.

Computing through the whole input data extracts a feature map of the data.

- Pooling layers: They reduce the sizes of the following layers by performing down-sampling through maximum pooling or average pooling operations, thereby reducing the computation time and complexity.
- Activation Unit: In this layer, a non-linear activation function is applied to each element in the feature space. The rectified linear unit (ReLU) activation function is selected in the majority of CNNs described in the literature. ReLU function can be mathematically described as $f(x) = max(0, x)$.
- Output Layer: In this layer, CNN estimates the output prediction.

A CNN-based network architecture is depicted in Fig. 9.

The work in [83] considers a CNN, an FNN, and a kNN approach to estimate the 3D position and the orientation of a randomly positioned light-fidelity (LiFi) PD receiver, without knowledge of the emitting power beforehand. Both ANNs leverage RSS fingerprints that include the received SNR. along with the corresponding orientation angles and coordinates. CNN obtains the best accuracy results, outperforming the other models, since the mean positioning error is 10.53 cm and all orientation angle estimations are below 10°. The ANN approaches outperform both the kNN model in terms of accuracy, bit error rate (BER), and computation time. In [9] various ML models (i.e., LR, ANN, and CNN) are employed to predict the 2D location of a PD, utilizing the DIALux lighting design software based on the AoA, and positioning unit cells, for a VLP system. CNN outperforms the other approaches, as the average positioning error is $3.83cm$, with ANN and LR also obtaining good positioning errors of 5.19 cm and 5.80 cm respectively. CNN, ANN, and LR approaches are compared in [89], along with preprocessing the RSS data values, to mitigate the light deficient regions in a VLP system, and estimate the 2D location of a PD target, along with the error distribution uniformity. CNN outperforms the other approaches, as the average positioning error, after pre-processing the data, is $5.31 \pm 3.84$ cm.

In [85] a combination of a ResNet and transfer learning (TL) is implemented, and compared to LR, to estimate the 2D position of a test-bed PD receiver. To obtain the RSS values, that are utilized as inputs in the approach, a scheme for duplicating a positioning unit cell model is developed and demonstrated experimentally. The proposed method outperforms the LR approach, with a mean average error of 6.69 cm and a standard deviation of 3.05 cm. Lin and Zhang in [77] apply a novel deep neural network (PE-DNN) to aid the VLC receivers, for user data recovery and position estimation, using channel impulse responses (CIRs) with pilot blocks. The PE-DNN method can accurately estimate the 2D coordinates of the receiver, with an average positioning error below 1 cm, by using only one PD receiver and one LED, keeping the remaining transceiver structures unchanged. Furthermore, the computation time is reduced, as the PE-DNN method performs an initial normalization of the pilot symbol P within the range of [0, 1].

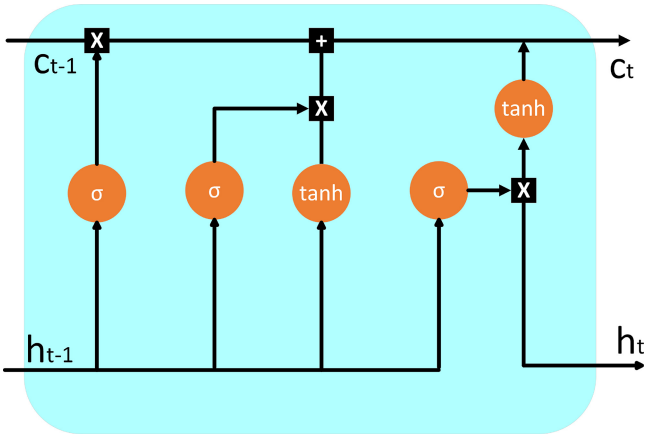


**FIGURE 10.** LSTM unit.

RNNs are a class of ANNs that process input data recurrently. They are used for processing tasks with sequential data input and learning the time-series relationship. The most widely used RNNs are LSTM, gated recurrent unit (GRU), and Bi-directional RNNs. Due to the back-propagation algorithm, RNNs had issues storing past information and learning the sequence for long-term dependencies. To solve the explicit memory issue, the LSTM method was developed. LSTM cell has the same inputs and outputs as a regular RNN but has more parameters and is composed of a gating system. The gating system contains an input gate, a forgetting gate, and an output gate that, during the training process, decides which information data to keep or drop based on the impact on predictions [139]. Fig. 10 shows an illustration of an LSTM unit.

Hsu et al. in [38] design a BP-based algorithm to improve the performance in 2D position estimation in a VLP system. The system utilizes several trilateral positioning cells to enfold the entire area of interest, taking into account the height fluctuation of the PD detector. RSS values are measured in unit cells for position estimation, and the BP method is utilized to adjust the positioning function parameters to improve accuracy, resulting in an average positioning error of 3.65 cm while demonstrating real-time tracking capabilities. In [72] the authors develop a modified momentum back-propagation (MMBP) approach to train an ANN for a 2D position estimation of a PD receiver, based on

RSS values. The MMBP algorithm achieves high-accuracy positioning and addresses the issue of sparse training data by combining two BP algorithms, namely momentum BP and variable learning rate BP, to enhance the convergence rate and generalization ability of the model. The MMBP method achieves an average positioning error of 1.99 cm, which outperforms conventional RSS-based localization approaches with a fast convergence rate.

In [76] the authors utilize a deep learning long short-term memory (DLSTM) approach for indoor localization, utilizing magnetic and light sensors in smartphone receivers. The DLSTM model takes pre-processed bimodal image data from the sensors to estimate the 2D position of the mobile camera receiver, with the average positioning error being 120 cm. As the computation time is $< 0.1$ s, the method used is suitable for real-time localization services. An LSTM network is compared in [57] with conventional FCN and SVR models in terms of 2D position estimation of a PD target in an indoor environment. The noise characteristics of the VLP system are analyzed and modeled as Gaussian white noise before inducing the RSS values as input to the ML models. The LSTM approach achieves the best accuracy results, with a mean positioning error of 0.92 cm. The authors of [90] compare LSTM with LR and ANN to estimate the 2D location of a silicon solar cell receiver, using only LED transmitters $T_x$ and a silicon-based solar cell $R_x$. The LSTM outperforms the other approaches in terms of positioning accuracy, with a mean percentage error of 2.9 cm, through the reduction of noise and the influence of time-dependent fluctuation.

A novel approach, namely AdVLP, is proposed in [80], to tackle both the challenge of estimating the 3D location of a PD receiver and the problem of data-driven methods being vulnerable to changes in channel parameters. The method is based on deep neural networks and uses adversarial training. The proposed generative adversarial network (GAN) can offer a significant improvement for the Lambertian orders of the receiver and the LED lights, as well as an improved average positioning accuracy $< 20$ cm.

#### 3) RL METHODS

Incorporating RL approaches into VLP systems can enhance their ability to provide precise location estimation and navigation. Various RL-based architectures (i.e., Q-learning and AC-based methods) have been included in this review. Q-learning is an RL value function algorithm that is based on the relationship of agent-environment, to create a Q-Table based on the reward action value. At a given time-step $t$ an agent of a state $\hat{S}_t$ tries to maximize the reward value $r$ through an action $\hat{A}_t$, The Q-Table of the model is constructed based on the updated Q-values $Q_{t+1}$ defined as [140]:

$$Q_{t+1}(\hat{S}_t, \hat{A}_t) \leftarrow (1-\delta)Q_t(\hat{S}_t, \hat{A}_t) + \delta(r_{t+1} + \epsilon \underset{\delta}{max} Q_t(\hat{S}_{t+1}, \delta)) \quad (13)$$

where $\delta$ is the step-size/learning rate, $\epsilon$ the discount factor for the future rewards, and $r$ is the reward value.

AC algorithm is a combination of Q-learning, a value-based optimization method, and policy-based optimization methods. The AC algorithm is based on an alternating loop between a PG "actor" algorithm to decide the action and a Q-learning-based "critic" model to evaluate the taken action, providing feedback to adjust the next actions based on the Q-value. The Q-value is obtained from the reward of the action and the next state of the environment [141].

The pros and cons of the studied ML methods in location estimation are included in Table 5, 6.

Iterative point-wise reinforcement learning (IPWRL) is proposed in [64] to predict the 2D location of a PD receiver based on the RSS values. IPWRL compensates the non-deterministic noise (i.e., shot noise, thermal noise) and deterministic noise, which can occur due to incorrect a priori knowledge of system parameters (i.e., the height difference between the receiver and LEDs). The IPWRL method corrects possible positioning errors caused by noises and enhances the mean positioning accuracy at 3.14 cm, at the cost of total running time due to the iterations. In [65] the authors present an AC-based approach for 3D position estimation without any offline training, where various AC-based models, which employ different height update strategies, are explored. The sequential combination of two strategies, namely $RL_1$ and $RL_2$. In $RL_1$ the RSS values are adjusted without changing the height difference $h$ between the PD receiver PD and LEDs, except for the last action. In $RL_2$ the RSS values and height $h$ are updated sequentially in each action. In the best method, namely $RL_3$ the RSS values and height are updated based on $RL_2$, and sequentially the $x, y$ coordinates are updated based on $RL_1$, obtaining an average positioning accuracy of 2.6 cm. Zhang et al. in [66] propose a Q-learning-based 2D positioning method utilizing a stereo camera system. The RL method aims to balance the handover rate and positioning accuracy, by segmenting the user's moving track at different speeds based on the rewards of the RL method. The proposed scheme is able to attain positioning precision at the millimeter level and enhance the normalized reward by over 40%, and decrease the handover rate by 87% and 78%, compared to the immediate handover (IHO) and dwell handover (DHO) approaches.

#### 4) EAS IN VLP FORMULATIONS

EAs have been widely used to resolve complex non-linear optimization problems, and their performance in VLP systems has received much attention in the last few years [112]. Various EAs have been investigated in the position estimation of receivers in VLC systems, and among the included research studies the most widely used are the genetic algorithm (GA) and particle swarm optimization (PSO).

GA is a population-based optimization algorithm that mimics Darwinian theory of biological evolution. The GA starts from a set of coded solutions satisfying a set of random constraints. The set formulates the initial population

**TABLE 5.** Advantages and limitations of ML algorithms used in VLP.

| Algorithm | Advantages | Limitations | References |
|---|---|---|---|
| Auto-encoders | Previous knowledge or information about the data is not required | Computational expensive | [142], [143] |
| | Efficient handling of large dimensional datasets | High complexity | |
| | Capable to comprehend nonlinear feature pattern in data | Too lossy | |
| kNN | Straightforward to apply in multi-class scenarios | Computational expensive | [143] |
| | One hyper-parameter (k) | Curse of dimensionality | |
| | Easy to understand and use without requiring extensive knowledge or expertise | Needs homogenous features | |
| Random Forest | High accuracy | High complexity | [143], [144] |
| | Performs well with limited data | Low correlation between trees | |
| | Robust | Necessary pruning | |
| k-means clustering | Easy to implement | Can cluster outliers | [143], [145] |
| | Easy adoption to new data | k greatly impacts performance | |
| | Suitable for large datasets | Initial scaling depends on number of dimensions | |
| DBSCAN | Suitable for arbitrary shape cluster | When the density of the data is low, clustering results have poor quality | [146], [147] |
| | Low complexity | Sensitive to high dimensional data | |
| Linear Regression | Simple to implement | Linear boundaries | [144] |
| | Regularization reduces overfitting | Outliers greatly impact performance | |
| | Easy to interpret | Assumes data independence | |
| CNN | Strong capabilities in feature extraction | High computational cost | [143] |
| | Weight sharing | GPU dependency | |
| | Easy to interpret | Large dataset needed | |
| ANNs | Can detect all potential interactions among predictive variables | Computationally intensive | [143], [148] |
| | Automatically identify intricate nonlinear connections between dependent and independent variables | Unexplained behavior of the network | |
| | Robust to noise | No rule for structure definition | |
| | Parallel processing capability | Lacks comprehension of the problem | |
| Gaussian proccess | Provide a full conditional statistical description for the predicted variable | High computational complexity | [149], [150] |
| | Non-parametric | Plain vanilla version | |
| | Obtain the model's uncertainty directly | Hierarchical feature extraction | |

$P_0$ based on an initialization method. In each generation (iteration), tentative solutions in the population are evaluated based on the fitness function to select the best adapted and remove the worst solutions. The GA generates new potential solutions $\bar{P}_g$ using variation operators such as mutation and crossover. These solutions are then evaluated using the fitness function in the main GA process. In the crossover operator, new solutions occur based on the exchange of genetic material, whereas in mutation, the genetic information of some solutions is modified. The newly

**TABLE 6.** Advantages and limitations of ML algorithms used in VLP (continued).

| Algorithm | Advantages | Limitations | References |
|---|---|---|---|
| ELM | Hidden layers' learning parameters do not have to be iteratively tuned | Linear boundaries | [151], [152] |
| | Good generalization performance | The learning parameters of the hidden layers' classification boundary not optimal | |
| | Non-linear transformation during training | Pseudo-inverse circulation | |
| | High learning speed | Random choise of input weights and biases | |
| SVM/SVR | High performance and accuracy | Long training time for large data-sets | [143], [153] |
| | Efficiently with non-linear data | Difficult to choose appropriate Kernel function | |
| | Good scaling and efficiency of high-dimensional data | The weights of the variables are not constant | |
| | Works well with unstructured data. | Poor performance with noise in data | |
| Actor critic | Low variance | Time consuming | [154], [155] |
| | More sample efficient compared other RL methods | Estimators need high variance | |
| | Trains value function based on ground-truth data | | |
| Q-learning | Relatively fast | Computationally expensive | [155], [156] |
| | Considers future actions | High-dimensionality issues | |
| | Learns directly the optimal policy | Use of biased samples | |

**Algorithm 1** Pseudo-Code of Standard GA

$g \leftarrow 0$
**Initialize** random population $P_0$
**Evaluate** the population $P_0$
**while** Termination criterion not satisfied **do**
  $\bar{P}_g \leftarrow variation(P_g)$
  **Evaluate** $(\hat{P}_g)$
  $\bar{P}_{g+1} \leftarrow replace(P_g, \bar{P}_g)$
  $g \leftarrow g + 1$
**end while**

generated solutions $\bar{P}_g$ replace the ones eliminated and, along with the current population $P_g$ of the generation, formulate the next generation population $P_{g+1}$. This process is repeated until convergence criteria, such as the quality of the solution and the maximum number of iterations, are satisfied. The last generation consists of the best solutions, in terms of the balance between fitness function and cost [157]. The pseudo-code of the standard GA is structured in Algorithm 1.

GA in VLC systems starts by formulating the search space of the parameters (i.e., position, RSS values, angles, etc.), and then by utilizing element randomization forms the initial population. By utilizing the survival of the fittest manner and mutation/crossover operations, the best individuals are combined to form the next generation. The fitness function of the GA in VLP systems is defined as the mean distance error of measured and projected positioning points. The evolution process is repeated until the best fitness value is achieved or the maximum number of generations / iterations is reached [101], [158]. The major advantages and limitations of the EAs for the position estimation of the VLP systems are included in Table 7.

PSO is a swarm intelligence algorithm and takes inspiration from the social behavior of bird flocks and fish schools. PSO is initialized with a population of random solutions, namely particles. Each particle $i$ in PSO flies through the search space and movement is adjusted based on both its own and its neighbor's behaviors and experiences. For each particle, a random velocity $v_i$ is generated. The positions of the initial population are randomly initialized based on the constraints of the problem and the movement of each particle is defined from an objective function $\mathscr{F}$. On the basis of the objective function, the optimal function value and location of each particle are determined. At each iteration, PSO updates the location and velocity of the particle according to the optimal location of each particle $P_i^{best}$ and its neighbors, as well as the current velocity until the stopping criterion is satisfied. Let $G_i^{best}$ represent the global best position of the group, then the updated position and velocity can be expressed as:

$$v_i(t+1) = v_i(t) + C_1 r_1 |P_i^{best}(t) - x_i(t)| + C_2 r_2 |G_i^{best}(t) - x_i(t)| \quad (14)$$

$$x_i(t+1) = x_i(t) + v_i(t+1) \quad (15)$$

**TABLE 7.** Advantages and limitations of EAs used in VLP.

| Algorithm | Advantages | Limitations | References |
|---|---|---|---|
| PSO | Easy to implement | Parameter tuning is required | [162], [163] |
| | Few parameters to adjust | Low convergence rate | |
| | Effective memory capability | Extensive computational time | |
| | Unsusceptible to variable scaling | Some techniques require binary conversion | |
| GA | Scalability | Unguided mutation operator | [164], [165] |
| | High degree of flexibility | Slow convergence speed | |
| | Easy to implement | Premature convergence | |
| DE | Simple and straightforward to implement | Struggle to solve large-scale optimisation problems | [166], [167] |
| | Low space complexity | Highly dependent on the control parameters | |
| | Guided mutation operator | Unstable convergence | |
| Bat algorithm | Equation between exploration and exploitation | Conventional searching performance | [168], [169] |
| | Maintains diversity | Low convergence speed | |
| | Able to handle multi-model problems efficiently | More parameter tuning is required | |
| Grey wolf optimizer | Easy implementation | Low exploitation ability | [170], [171] |
| | Supports distributed parallel computing | Slow convergence in the later stage | |
| | Fewer parameters that do not require fine-tuning | Low solution accuracy | |

$u_i$ is the particle's velocity, $x_i$ the particle's position, $C_1$ and $C_2$ the cognitive and social acceleration learning coefficient and $r_1$ and $r_2$ are random values within [0, 1] [159], [160].

In VLP systems, PSO is based on RSS signal values, with each particle representing a candidate for the position of the receiver. Each location receives RSS signals from all transmitters. Furthermore, various velocity speeds are initialized to the corresponding particles, and the predicted RSS value is compared with the real-time signal, to minimize the loss function. The loss function corresponds to the average distance error between the real and estimated location points. The process is repeated until the optimal position and velocity are determined based on the objective function [110], [161].

PSO is proposed in [108] in a 5G VLP system to extract the positioning reference signal (PRS) and improve the 2D positioning accuracy of an SVM through the subcarrier selection. An SVM is employed using the PRSs that have the lowest positioning error and the corresponding subcarrier sequence numbers as input. This approach results in an accuracy improvement of 73.28% and an average 2D positioning error of less than 6$cm$ for the PD sensor. In [110] PSO is applied to estimate the location of a PD target based on RSS values from the transmitters by updating the group's optimal location. An ANN used the estimation of the PSO combined with the RSS data to refine the estimation and accurately predict the real-time location of the receiver, with a mean 3D positioning error of 10$cm$, while offering 3 times wider coverage. In [114] PSO is studied to determine the optimal position of an RIS array to maximize the achievable rate performance, based on PD sensors.

In [93] a positioning approach based on a modified PSO algorithm improved by simulated annealing (SA), that is, simulated annealing particle swarm optimization (SA-PSO). The algorithm estimates the 3D location by using the unique signals transmitted by each LED and analyzing the messages received by the PD receiver terminal. Kalman filters have been utilized to suppress interference signals, improving accuracy and reducing computation time, with an experimental average 3D positioning error of 3.492$cm$. The authors in [94] implement a chaotic particle swarm optimization algorithm (CPSO) for a VLC-based 3D indoor positioning system. Chaos optimization utilizes the properties of randomness, ergodicity, and regularity of variables to perform a direct search and optimize the search process. The approach involves linearly mapping chaotic variables to the PD target location interval and utilizing them to efficiently search for the global optimal solution, thus it is time-consuming. PSO is combined with chaos optimization to leverage and find a better initial value, with the final position being estimated based on the carrier search of the chaos algorithm, obtaining an average 3D positioning accuracy of 1.4 cm, and reducing complexity. A PSO approach is employed in [102] to obtain the optimal configuration of a fuzzy-based 2D localization system. The suggested fuzzy-based approach expands the concept of trilateration by eliminating the requirement of solving multiple equations to determine the PD sensor's location. The PSO is applied to optimize the membership functions of the fuzzy logic

controller, and by performing range adjustment, localization reliability is achieved, with a mean positioning error of 43 cm.

A 3D VLP positioning method based on adaptive parameter particle swarm optimization (AP-PSO), namely adaptive mutation parameter particle swarm optimization (AP-PSO-M) is developed in [105]. The proposed AP-PSO-M algorithm takes into account both the LOS model, which is affected by noise interference, and the NLOS model, which is affected by multipath reflections. It has an advantage over the standard PSO algorithm, as it is less likely to get trapped in a local optimal solution. Additionally, the approach requires less computational complexity, since it only uses half of the swarm compared to the standard PSO algorithm. The average 3D positioning error achieved with this algorithm is 16.59 cm, even without prior knowledge of the height of the PD receiver. In [107] an improved particle swarm optimization (IPSO) algorithm is applied to produce the most efficient layout design that jointly maximizes both the positioning accuracy and the ergodic capacity of the VLC/VLP system. The IPSO is developed on the basis of a new metric, namely entropy of positioning (EOP), to evaluate positioning accuracy based on the concept of entropy in information theory. IPSO obtains a layout pattern to minimize the ergodic EOP, based on the RSS values, with the average 2D positioning error of the PD target, being below 50 cm.

A variation of IPSO based on the Min-Max algorithm, namely IPSO-Min-Max is studied in [113], to ensure that particles are always in close proximity to the target. The proposed method utilizes a nonlinear decreasing strategy for the inertia weight, based on the Bessel filter, to ensure stable particle velocity during the iterative process. As a result, the average positioning error of the PD target is less than 4 cm. However, to achieve a smaller positioning delay, the accuracy is reduced. Chen et al. in [109] utilize an improved immune particle swarm optimization (IIPSO) algorithm for high-precision position estimation in a 3D indoor environment. Monte Carlo ray tracing is used to analyze the effect of multipath reflections, and the optimal viewing angle of the PD receiver is determined to minimize the impact of the reflections. Also, by utilizing Kalman filters, the received light power from the LEDs is optimized, and by enhancing the inertial coefficient and the acceleration factor, the IIPSO achieves a 3D positioning accuracy of 3.12 cm, with a shorter average convergence rate of 2 s.

GA is utilized in [101] to estimate the 2D location of a receiver, consisting of a position-sensitive detector (PSD) PD and a coupled lens. A novel method in which a PSD PD onboard of a mobile target, followed by geometric calibration, is utilized to obtain the AoA of the received signals. The locations of the points of impact in relation to the PSD system's environmental position are used as inputs to the GA, to provide intrinsic/extrinsic parameters and the precise location of the emitters. The proposed method obtains an average 2D position error $<$ 4.5 cm,

**Algorithm 2** Pseudo-Code of Standard PSO

**Initialize** population size $S$, and maximum generation $t_max$
**for** $i = 1 : S$ **do**
  Generate randomly $x_i$ and $v_i$
  $P_i = x_i$
**end for**
**Set** $G^{best} = P_1^{best}$ & $f(G^{best}) = f(P_1^{best})$
**for** $i = 1 : S$ **do**
  **if** $f(P_i^{best}) < f(G^{best})$ **then**
    $f(G^{best}) = f(P_i^{best})$
  **end if**
**end for**
**while** Termination criterion not satisfied & $t < t_{max}$ **do**
  **for** $i = 1 : S$ **do**
    **Update** velocity using (14)
    **Update** position using (15)
    **if** $f(x_i(t+1)) < f(P_i^{best})$ **then**
      $P_i^{best} = x_i(t+1)$
      $f(P_i^{best}) = f(x_i(t+1))$
    **end if**
    **if** $f(P_i^{best}) < f(G^{best})$ **then**
      $G^{best} = P_i^{best}$
      $f(G^{best}) = f(P_i^{best})$
    **end if**
  **end for**
  $t \leftarrow t + 1$
**end while**
**return** $G^{best}$

without prior knowledge of the system parameters. In [117] apply GA to obtain a low-complexity, weak calibration for an indoor VLP system. The suggested calibration only needs six measurement locations inside the environment, and via the GA the calibration constants are obtained, without knowing the system characteristics beforehand. The weak calibration technique improves the accuracy of position and orientation estimation using a PSD that measures the angle of arrival from modulated infrastructure lighting. The mean 3D positioning error is reduced to 35 mm and the orientation angle errors are around 0.25°. The authors in [104] prepare a comparison of GA and PSO in terms of 2D position estimation and boundary limitations. GA outperforms PSO in terms of PD receiver position estimation accuracy, for the upper bounded optimization problem, the average error is 12 cm, has a lower deviation, and is more robust.

In [92] a 3D position estimation method, based on a modified genetic algorithm (MGA) is developed. The MGA approach can achieve an average localization error of $<$ 1.02 cm, without the need to presume the height or the orientation angle of the mobile PD device. The approach considers the first-order reflection and employs an ANN to match the model of a nonlinear channel, reducing the average positioning errors at the four corners from 11.94 cm

to 0.95 cm. MGA is also studied in [98] to improve the precision of a reversed indoor 3D positioning system. The positioning problem is treated as a multi-parameter optimization problem, and the global parallel search of MGA is utilized. By optimizing the attenuation factor in RSS values and incorporating the error correction factors into MGA, the 3D average positioning accuracy of the PD sensor is improved to 2.32 cm. An improved genetic algorithm (IGA) is applied in [116] to enhance performance in positioning accuracy in a VLP system. In this scheme, a single LED and four-quadrant PDs are utilized as light source transmitters and receivers, to accurately estimate the location of measured points, with the average 3D positioning error $< 4$ cm. IGA can obtain better positioning accuracy and robustness, compared with the standard GA.

In [91] ACO utilizes the global search property to identify the optimal PD location point, and the parallel search property to correct the deviation of the intensity attenuation factors, with the average 3D positioning error at 2 cm, 4 cm, and 8 cm when SNR is 30 dB, 20 dB, and 10 dB, respectively. Authors in [95], [96] transform the 3D positioning problem of a PD target, into a global optimization problem, and a fitness function is developed based on the Lambertian radiation pattern to achieve higher accuracy and lower system complexity. The positioning problem can be addressed with MFOA, where the strategy of the fly group in the traditional fruit fly optimization algorithm is altered, and an adaptive search scope is utilized to obtain an average 3D positioning accuracy of 0.76 cm. Also, AFSA can offer excellent accuracy results in indoor 3D positioning problems, as the average error for a moving target is 3.57 mm.

The paper [97] proposes a global optimization approach to solve the 3D positioning of a PD node, by computing the area of overlap of circular projections of LEDs on the terminal plane. Differential Evolution (DE) is used to optimize the fitness function and determine the Z-coordinate of the terminal. DE also reduces the dimensionality of the problem from 3D to one-dimensional (1D), which significantly improves the computation time. The average 3D positioning error is 0.69 cm within an indoor environment of with a reduced computation time of 24.26 ms per single point. The RSS-based simultaneous positioning and orientating (SPAO) problem is addressed in [99] with a novel multi-scale particle-assisted stochastic search (PASS) algorithm. The PASS algorithm has an average 3D positioning error of the PASS algorithm is 10 cm and an orientation error of 70 cm, in an affordable computational time of 2 s. The PASS-based solution can be utilized for practical VLC localization systems, as for the accurate position estimation prior knowledge concerning the PD receiver's height, the precise alignment of transceiver orientations, or the use of inertial measurements is not required. Peng et al. in [100] propose the TSA to estimate the 3D location of a PD, for both static and dynamic trajectory positioning. As TSA emulates the human memory mechanism, it can avoid being stuck in local minima and enables a wider search space exploration, offering average 3D position error below 1.791 cm and 1.428 cm for static and dynamic positioning respectively.

In [103] is applied as a global optimization method to solve the 3D position estimation of a PD sensor target. BA is inspired by microbats' echolocation ability to navigate around obstacles and locate prey in low-light conditions. As micro-bats pursue prey, they decrease the volume of their emitted ultrasonic sounds but increase the emission rate. The position of the receiver is predicted by identifying the bat within the entire population that has the lowest value of the fitness function. The BA approach provides a good balance between complexity and accuracy, with an average error of 2.12 cm in 3D positioning. A variant of BA, namely the improved hybrid bat algorithm (IHBA), is studied in [106] to improve the performance of 3D position estimation in a VLC system while considering the tilt of the receiver. IHBA incorporates several features to enhance its performance. A set of beacon points are established at the outset to reduce the number of iterations required, while the fitness function includes a weight coefficient to improve positioning accuracy. The algorithm introduces an adaptive search factor to regulate the speed of the bat individual update process. A chaotic perturbation operation is utilized to avoid the algorithm from getting stuck in local optima. As a result, the algorithm achieved an average positioning error of 3.64 cm and a quicker convergence rate of 0.89 seconds.

The improved adaptive cuckoo search algorithm (IACSA) [111] and the improved whale optimization algorithm (IWOA) [112] are also studied to improve the positioning accuracy in VLP systems, while considering the rotation angles of the PD receiver. In [111] for kinematic positioning without PD rotation, the average 3D positioning error is 1.54 cm and, in the case of PD rotation, 16.48 cm. The IWOA applied in [112] has elite opposition-based learning and Lévy flight strategy. PD rotation is considered and the average 3D positioning error is 7.85 cm, and 27.14 cm when angle estimation is ignored and taken into account, respectively.

In [118] the input weights and hidden biases of an ELM are optimized using gray wolf optimization (GWO) and particle swarm optimization (PSO). These optimization methods incrementally update the randomly initialized parameters, enhancing the 3D positioning accuracy. GWO-ELM outperforms ELM-PSO, as the average positioning error is 6.49 cm versus 6.90 cm. Both GWO and PSO offer a significant improvement of 58.16% and 55.51% in 3D environments while reducing the computational complexity of the problem. GWO is also applied in [115] combined with the non-sorting genetic algorithm III (NSGA-III), to formulate a multiobjective optimization strategy that maximizes power and spectral efficiency in a VLP system and utilizes an LSTM to predict PD positions, based on the optimal solutions of the HMO process. The proposed method obtains a reduction of 80% in power consumption and 20% in spectrum bandwidth. Based on the optimal parameters of the

**TABLE 8.** kNN methods included in the review.

| References | Approach | Positioning error | Setup | Environment | Sensor | Test size area | Method | LED Number |
|---|---|---|---|---|---|---|---|---|
| [42] | kNN | 2 cm | Simulation | 2D | PD | 5 m x 5 m x 3 m | Fingerprints | 4 |
| [40] | wkNN | 2.7 cm | Experiment | 2D | PD | 3.3 m x 2.1 m x 2.4 m | Fingerprints | 4 |
| [52] | WokNN | 8 mm | Simulation | 2D | PD | 1.2 m x 1.2 m x 1.2 m | Fingerprints | 4 |
| [54] | wkNN | 12 cm | Experiment | 2D | PD | 3.4 m x 3.4 m x 2 m | Fingerprints | – |
| [16] | wkNN | 1.92 cm | Experiment | 2D | PD | 5 m x 5 m x 5 m | Fingerprints | 4 |
| [55] | wkNN | 4.74 mm | Experiment | 2D | PD | 1.2 m x 1.2 m x 1.6 m | Fingerprints | 4 |
| [49] | WCkNN | 195 cm | Experiment | 2D | PD | 1.5 m x 4.4 m x 7.6 m | Fingerprints | 4 |

**TABLE 9.** ANN methods included in the review.

| References | Approach | Positioning error | Setup | Environment | Sensor | Test size area | Method | LED Number |
|---|---|---|---|---|---|---|---|---|
| [68] | MLP | 1.9 cm | Simulation | 2D | Camera | 1.3 m x 1.3 m x 2 m | Proximity | 5 |
| [67] | ANN | 1.66 cm | Experiment | 2D | PD | 5 m x 5 m x 3 m | Trilateration | 4 |
| [69] | MLP | 0.4 mm | Simulation | 3D | PD | 4 m x 4 m x 3 m | Fingerprints | 16 |
| [79] | MLP | $<$ 10 cm | Experiment | 2D | PD | 12 m x 18 m x 6.81 m | Fingerprints | 8 |
| [71] | ANN | 0.9 cm | Simulation | 3D | PD | 0.9 m x 0.9 m x 2.7 m | Trilateration | 3 |
| [25] | ANN | 11.93 cm | Experiment | 3D | PD | 1.2 m x 1.2 m x 2 m | Trilateration | 3 |
| [74] | ANN | 1 cm | Simulation | 3D | PD | 4 m x 4 m x 2.5 m | Triangulation | 4 |
| [75] | ANN | 0.73 cm | Experiment | 2D | PD | 0.5 m x 0.6 m x 0.1 m | Fingerprints | 2 |
| [78] | ANN | 2.98 cm | Experiment | 3D | PD | 5 m x 5 m x 5 m | Other method | 2 |
| [82] | Memory ANN | 3.53 cm | Experiment | 3D | PD | 0.6 m x 0.6 m x 1.4 m | Triangulation | 3 |
| [88] | ANN | 2 cm | Simulation | 2D | PD | 6 m x 6 m x 3 m | Other method | 4 |
| [84] | ANN | 80 cm | Simulation | 2D | PD | 5 m x 5 m x 3 m | Other method | 9 |
| [81] | ANN | 0.65 cm | Experiment | 3D | Camera | 4 m x 4 m x 3 m | Triangulation | 4 |
| [53] | ANN | 2.6 cm | Experiment | 2D | PD | 6 m x 6 m x 3 m | Trilateration | 4 |

**TABLE 10.** Deep learning architectures included in the review.

| References | Approach | Positioning error | Setup | Environment | Sensor | Test size area | Method | LED Number |
|---|---|---|---|---|---|---|---|---|
| [73] | Bayesian regularization DNN | 4.58 cm | Experiment | 2D | PD | 1.8 m x 1.8 m x 2.1 m | Trilateration | 4 |
| [83] | CNN | 10.53 cm | Simulation | 3D | LiFi PD | 5 m x5 m x 3 m | Fingerprints | 16 |
| [9] | CNN | 3.83 cm | Simulation | 2D | Solar cell | 0.4 m x 0.4 m x 1 m | Triangulation | 1 |
| [89] | CNN | 5.31 $\pm$ 3.84 cm | Experiment | 2D | PD | 1.5 m x 2 m x 2.5 m | Trilateration | 4 |
| [85] | ResNet | 6.69 $\pm$ 3.05 cm | Experiment | 2D | PD | 5 m x 5 m x 2.8 m | Other method | 6 |
| [87] | Two-stage neural network | 10 cm | Experiment | 3D | PD | 2 m x 1.5 m x 3 m | Other method | 4 |
| [77] | Position-estimation DNN | $<$ 1 cm | Simulation | 2D | PD | 5 m x 4 m x 3 m | Other method | 2 |
| [76] | Deep learning LSTM | 120 cm | Experiment | 2D | Camera | 8 m x 20 m x h | Fingerprints | 10 |
| [57] | LSTM | 0.92 cm | Experiment | 2D | PD | 1 m x 1.1 m x 1.75 m | Fingerprints | 1 |
| [90] | LSTM | $\sim$ 2.9 cm | Experiment | 2D | Solar cell | 0.4 m x 0.4 m x 1 m | Triangulation | 1 |

HMO, that offer these reductions, the LSTM has an average 2D positioning error of $<$7%.

### 5) COMPARISON

The analysis presented in the above sections is summarized in Tables 8 - 14. Information about the approaches and the use-case scenario (i.e., setup, environment, sensor type, size of test area, method, number of LEDs), and their optimal results in terms of accuracy and positioning error, are included. Tables 8 - 11 depict the performance of ML, DL and RL approaches in terms of position estimation in VLP systems, whereas Tables 12 - 14 show the EA accuracy

**TABLE 11.** Other ML methods included in the review.

| References | Approach | Positioning error | Setup | Environment | Sensor | Test size area | Method | LED Number |
|---|---|---|---|---|---|---|---|---|
| [39] | Linear regression | 40 cm | Simulation | 3D | PD | 5 m x 5 m x 4 m | Fingerprints | 8 |
| [56] | Linear regression | 11.1 cm | Experiment | 2D | PD | 2 m x 1.5 m x 2.7 m | Fingerprints | 4 |
| [50] | Ridge regression | 3 cm | Experiment | 2D | Camera | 0.4 m x 0.4 m x h | Triangulation | 4 |
| [11] | Ridge regression | 2.06 cm | Experiment | 3D | PD | 1 m x 1 m x 2.7 m | Fingerprints | 4 |
| [44] | Random forest | 10 cm | Experiment | 3D | PD | 2 m x 2 m x 3 m | Trilateration | 4 |
| [41] | Decision tree | 11 cm | Experiment | 2D | PD | 0.75 m x 0.1 m x 1.25 m | Fingerprints | 16 |
| [42] | Random forest | 2 cm | Simulation | 2D | PD | 5 m x 5 m x 3 m | Fingerprints | 4 |
| [62] | Decision tree | 3.8 cm | Simulation | 3D | PD | 5 m x 5 m x 3 m | Triangulation | 100 |
| [6] | Gaussian process | 7.17 cm | Experiment | 2D | PD | 4 m x 4 m x h | Trilateration | 4 |
| [51] | Gaussian process | 2 cm | Experiment | 2D | PD | 3 m x 2 m x 2 m | Trilateration | 4 |
| [8] | Gaussian process | $<$ 10 cm | Experiment | 2D | PD | 6 m x 4 m x 6 m | Other method | 4 |
| [59] | Gaussian process | 16.65 cm | Experiment | 2D | PD | 3 m x 3 m x 1.3 m | Triangulation | 4 |
| [61] | Generalized Gaussian distribution | N/A | Experiment | 2D | PD | 4.8 m x 5.4 m x 0 m | Trilateration | 4 |
| [39] | k-means clustering | 40 cm | Simulation | 3D | PD | 5 m x 5 m x 4 m | Fingerprints | 8 |
| [46] | k-means clustering | 31 cm | Experiment | 2D | PD | 4.3 m × 4 m × 4 m | Proximity | 2 |
| [60] | DBSCAN + ELM | 1.74 cm | Simulation | 3D | PD | 4 m x 4 m x 3.1 m | Other method | 1 |
| [47] | DBSCAN | 3.5 cm | Simulation | 2D | PD | 4 m x 4 m x 2.5 m | Trilateration | 25 |
| [70] | Convolutional auto-encoder | 4.68 cm | Simulation | 2D | Camera | 20 m x 15 m x 3 m | Fingerprints | 20 |
| [38] | Back-propagation | 3.65 cm | Experiment | 2D | PD | 1 m x 1 m x 2.5 m | Trilateration | 3 |
| [72] | Modified back-propagation | 1.99 cm | Simulation | 2D | PD | 1.8 m x 1.8 m x 2.1 m | Fingerprints | 4 |
| [63] | ELM | 3 cm | Experiment | 3D | PD | 0.2 m x 0.2 m x 1.8 m | Fingerprints | 4 |
| [64] | Iterative point wise RL | 3.14 cm | Experiment | 2D | PD | 1.2 m x 1.2 m x 1.2 m | Trilateration | 4 |
| [65] | Actor critic | 2.6 cm | Experiment | 3D | PD | 1.2 m x 1.2 m x 2.2 m | Trilateration | 4 |
| [66] | Q-learning | mm-level | Experiment | 2D | Camera | 15 m x 21 m x 3 m | Other method | 24 |
| [80] | GAN | $<$ 20 cm | Experiment | 3D | PD | 6 m x 5 m x 2.8 m | Fingerprints | 5 |
| [37] | Grid-dependent least square | 5 cm | Experiment | 2D | PD | 3 m x 2 m x 2.5 m | Fingerprints | 4 |
| [58] | Co-training regression and adaptive boosting | 2.51 cm | Experiment | 2D | PD | 1.2 m x 1.2 m x 1.2 m | Fingerprints | 96 |
| [45] | Two layer-fusion network | 5 cm | Experiment | 2D | PD | 3 m x 2 m x 2.5 m | Fingerprints | 4 |
| [43] | SVM | 8.6 cm | Simulation | 2D | PD | 5 m x 5 m x 2.5 m | Trilateration | 4 |
| [48] | 2nd order regression | 4 cm | Simulation | 2D | PD | 4 m x 4 m x 4 m | Trilateration | 3 |

in the various scenarios and systems. In most of the included works, PD sensors are utilized as receivers and target nodes, with a few camera-based and solar cell-based approaches. Furthermore, the measurement methodology is included, with most of the included paper utilizing fingerprints and trilateration methods. Triangulation is also studied in some works, whereas proximity is scarcely utilized in these works. Some authors study the positioning problem by exploiting other methods (e.g., receiver diversity unit cell duplication, RSS measurements) to provide their AI-based localization approach, especially for the EA methodology. It is worth mentioning that in some works, authors did not give any information on the height of the test area, thus h value was assigned.

## V. OPEN CHALLENGES AND CONCLUSION

This methodological review aimed to provide a comprehensive overview of AI-based VLP studies. ML and nature-inspired evolutionary research works have been analyzed, during the last six years in different environments (2D/3D) and methods (experiment/simulation). AI methods are capable of enhancing performance and robustness in predicting receiver position, but there are still some unresolved challenges in the field, analyzed in Section V-A.

### A. OPEN CHALLENGES AND FUTURE DIRECTIONS

The use of AI methods may offer robust and reliable results, but there are still challenges to be addressed in indoor positioning systems, including VLC configurations [172]:

**TABLE 12.** PSO approaches included in the review.

| References | Approach | Positioning error | Setup | Environment | Sensor | Test size area | Method | LED Number |
|---|---|---|---|---|---|---|---|---|
| [93] | Simulated annealing PSO | 3.49 cm | Experiment | 3D | PD | 3 m × 3 m × 4 m | Other method | 4 |
| [94] | Chaotic PSO | 3 × 3 × 4 | Simulation | 3D | PD | 3 m × 3 m × 4 m | Trilateration | 3 |
| [102] | Fuzzy PSO | 43 cm | Experiment | 2D | PD | 60 m× 40 m × 14 m | Trilateration | 10 |
| [105] | Adaptive mutation parameter PSO | 16.59 cm | Simulation | 3D | PD | 4 m × 4 m × 3 m | Other method | 4 |
| [107] | Improved PSO | $<$ 50 cm | Simulation | 2D | PD | 5 m × 5 m × 3 m | Other method | 3 |
| [108] | PSO | $<$ 6 cm | Experiment | 2D | PD | 0. 3 m × 0.3 m × 2.14 m | Trilateration | 4 |
| [109] | Improved Immune PSO | 3.12 cm | Simulation | 3D | PD | 5 m × 5 m × 5 m | Other method | 9 |
| [110] | PSO | 10 cm | Simulation | 3D | PD | 5 m × 5 m × 3 m | Other method | 4 |
| [113] | IPSO-Min-Max | $<$ 4 cm | Simulation | 3D | PD | 4 m × 4 m × 4 m | Other method | 3 |
| [114] | PSO | – | Simulation | 2D | PD | 5 m × 5 m × 3 m | Other method | 1 |

**TABLE 13.** GA methods included in the review.

| References | Approach | Positioning error | Setup | Environment | Sensor | Test size area | Method | LED Number |
|---|---|---|---|---|---|---|---|---|
| [92] | Modified GA | $<$ 1.02 cm | Simulation | 3D | PD | 3 m× 3 m × 4 m | Fingerprints | 4 |
| [98] | Modified GA | 2.32 cm | Experiment | 3D | PD | 3 m× 3 m × 4 m | Trilateration | 4 |
| [101] | GA | $<$ 4.5 cm | Experiment | 2D | PD | 3 m × 3 m × 3 m | Other method | 3 |
| [104] | GA | 12 cm | Simulation | 3D | PD | 1.4 m × 1.4 m × 3 m | Other method | 4 |
| [116] | Improved GA | $<$ 4.02 cm | Experiment | 3D | PD | 4 m × 4 m × 6 m | Other method | 4 |
| [117] | GA | 35 mm | Experiment | 3D | Position detector | 7 m x 4 m x 2.5 m | Triangulation | 4 |

**TABLE 14.** Other EAs included in the review.

| References | Approach | Positioning error | Setup | Environment | Sensor | Test size area | Method | LED Number |
|---|---|---|---|---|---|---|---|---|
| [91] | Ant colony optimization | 2 cm | Simulation | 3D | PD | 3 m x 3 m x 4 m | Other method | 4 |
| [95] | Modified fruit fly optimization algorithm | 0.76 cm | Simulation | 3D | PD | 4 m × 4 m × 6 m | Trilateration | 4 |
| [96] | Artificial fish swarm algorithm | 3.57 mm | Simulation | 3D | PD | 4 m × 4 m × 6 m | Other method | 4 |
| [97] | DE | 0.69 cm | Experiment | 3D | PD | 4 m × 4 m × 6 m | Trilateration | 4 |
| [99] | Particle-assisted stochastic search | 10 cm | Simulation | 3D | PD | 9 m × 9 m × 4 m | Trilateration | 81 |
| [100] | Tabu search | 1.43 cm | Simulation | 3D | PD | 3 m × 3 m × 4 m | Other method | 4 |
| [103] | Bat algorithm | 2.12 cm | Simulation | 3D | PD | 3 m × 3 m × 4 m | Other method | 4 |
| [106] | Improved hybrid bat algorithm | 3.64 cm | Experiment | 3D | PD | 1.5 m × 1.2 m × 2 m | Other method | 4 |
| [111] | Improved adaptive cuckoo search algorithm | 1.54 cm | Simulation | 3D | PD | 5 m × 5 m × 6 m | Other method | 4 |
| [112] | Improved whale optimization algorithm | 2.14 cm | Simulation | 3D | PD | 5 m × 5 m × 6 m | Fingerprints | 4 |
| [115] | Grey wolf optimization | $<$ 7% | Simulation | 2D | PD | 8 m × 6 m × 4 m | Other method | 1 |
| [118] | Grey wolf optimization | $<$ 6.49 cm | Experiment | 3D | PD | 2 m × 2 m × 2.5 m | Fingerprints | 4 |

- Data availability: The quantity and quality of the data greatly impact the accuracy and performance of AI methods. Estimating and measuring the required data is a tough task, and also the collected data may present divergences caused by the device heterogeneity.

- Computation time and complexity: AI-based approaches require different training and estimation times, depending on the problem and the system model. Complex models may offer better accuracy results, but optimizing complexity and performance is essential.
- Variability shortage: AI models can provide accurate predictions based on the available data. However, it is hard to ascertain that the models are suitable for all use case scenarios.
- Environment: AI methods can offer accurate and robust results for IPs, but their performance may differ in less ideal environments, such as underwater or underground scenarios.
- RSS-based VLP heavily relies on the predictability of the visible light channel. In comparison with sub-GHz RF propagation, the visible light channel can be modeled much more precisely [173], [174], [175], leading to a higher accuracy of RSS-based positioning. The main reason is that RSS-based VLP does not suffer from small-scale fading. Moreover, it was shown that reflections have a smaller (and more deterministic) impact [176]. This also explains why reflections have not frequently been researched, as positioning only accounting for the LoS contributions already yields good accuracy.

Telecommunication engineering has made significant progress, leading to the development of improved VLC technologies and services. The VLC community has identified several research directions that show promise for future development, including [21], [177], [178]:

- The advancement in high-speed complementary metal-oxide-semiconductor (CMOS) image sensors (ISs) is crucial in enhancing the accuracy of indoor localization systems that employ deep learning. The evolution of IS technology, since LEDs are increasingly becoming the preferred lighting option in IPs, can enable smartphones, which are already ubiquitous, to become the primary devices for indoor positioning problems.
- Integration with other wireless technologies: Combining VLP with other wireless technologies such as WiFi, Bluetooth, or ultra-wideband can enhance the accuracy and reliability of indoor positioning systems.
- Real-time positioning: Real-time positioning using VLP systems can improve applications such as indoor navigation, emergency response, and location-based services.
- Outdoor Positioning: Outdoor positioning is a very complex and attractive challenge, as it is difficult for PDs to deploy in an outdoor environment, and environmental factors greatly impact their performance. The use of off-camera receiving systems in outdoor positioning can offer solutions in future networks.
- Hybrid positioning: The combination of VLP with other positioning technologies, such as GPS or sensor fusion, can improve the accuracy of outdoor and indoor positioning systems.
- Vehicular communications: Every vehicle is equipped with high-power head and tail lights. Also, light waves can be more reliable than radio frequency signals in closed spaces; thus, VLC and VLP based on cameras can offer various solutions in the future of vehicular communications and vehicle-to-vehicle (V2V) positioning.

### B. CONCLUSION

VLP technology can achieve highly accurate real-time localization in indoor IoT networks, compared to RF-based positioning systems, thus playing a vital role in the much needed precise tracking of IoT devices. Combining AI and VLP can offer highly accurate positioning services in indoor IoT systems, which are essential in the upcoming future wireless networks. In this methodological review, a discussion of AI methods concerning position estimation in VLC systems for indoor IoT applications is conducted. Relevant studies published in peer review journals or conferences in the last six years are included in this work. The use of AI in IPs and especially the VLC-based system is a growing trend to improve localization services. AI methods offer the flexibility to be combined with conventional localization techniques and enhance accuracy and robustness, thus posing as a promising candidate to improve VLC localization services for indoor IoT applications.

## REFERENCES

[1] B. Khalfi, B. Hamdaoui, and M. Guizani, "Extracting and exploiting inherent sparsity for efficient IoT support in 5G: Challenges and potential solutions," *IEEE Wireless Commun.*, vol. 24, no. 5, pp. 68–73, Oct. 2017.

[2] N. Saxena, A. Roy, B. Sahu, and H. Kim, "Efficient IoT gateway over 5G wireless: A new design with prototype and implementation results," *IEEE Commun. Mag.*, vol. 55, no. 2, pp. 97–105, Feb. 2017.

[3] H. Yang et al., "Coordinated resource allocation-based integrated visible light communication and positioning systems for indoor IoT," *IEEE Trans. Wireless Commun.*, vol. 19, no. 7, pp. 4671–4684, Jul. 2020.

[4] M. Keskin, A. Sezer, and S. Gezici, "Localization via visible light systems," *Proc. IEEE*, vol. 106, no. 6, pp. 1063–1088, Jun. 2018.

[5] L. Wan, G. Han, L. Shu, S. Chan, and N. Feng, "PD source diagnosis and localization in industrial high-voltage insulation system via multimodal joint sparse representation," *IEEE Trans. Ind. Electron.*, vol. 63, no. 4, pp. 2506–2516, Apr. 2016.

[6] N. Knudde, W. Raes, J. De Bruycker, T. Dhaene, and N. Stevens, "Data-efficient Gaussian process regression for accurate visible light positioning," *IEEE Commun. Lett.*, vol. 24, no. 8, pp. 1705–1709, Aug. 2020.

[7] F. Alam, N. Faulkner, and B. Parr, "Device-free localization: A review of non-RF techniques for unobtrusive indoor positioning," *IEEE Internet Things J.*, vol. 8, no. 6, pp. 4228–4249, Mar. 2021.

[8] F. Garbuglia, W. Raes, J. De Bruycker, N. Stevens, D. Deschrijver, and T. Dhaene, "Bayesian active learning for received signal strength-based visible light positioning," *IEEE Photon. J.*, vol. 14, no. 6, Dec. 2022, Art. no. 8559208.

[9] H. M. Chan et al., "Utilizing lighting design software for simulation and planning of machine learning based angle-of-arrival (AOA) visible light positioning (VLP) systems," *IEEE Photon. J.*, vol. 14, no. 6, Dec. 2022, Art. no. 7358407.

[10] N. Chi, Y. Zhou, Y. Wei, and F. Hu, "Visible light communication in 6G: Advances, challenges, and prospects," *IEEE Veh. Technol. Mag.*, vol. 15, no. 4, pp. 93–102, Dec. 2020.

[11] Y.-C. Wu et al., "Received-signal-strength (RSS) based 3D visible-light-positioning (VLP) system using kernel ridge regression machine learning algorithm with sigmoid function data preprocessing method," *IEEE Access*, vol. 8, pp. 214269–214281, 2020.

[12] A. B. M. M. Rahman, T. Li, and Y. Wang, "Recent advances in indoor localization via visible lights: A survey," *Sensors*, vol. 20, no. 5, p. 1382, 2020.

[13] H. Obeidat, W. Shuaieb, O. Obeidat, and R. Abd-Alhameed, "A review of indoor localization techniques and wireless technologies," *Wireless Pers. Commun.*, vol. 119, no. 1, pp. 289–327, 2021.

[14] S. Bastiaens et al., "Experimental benchmarking of next-gen indoor positioning technologies (unmodulated) visible light positioning and ultra-wideband," *IEEE Internet Things J.*, vol. 9, no. 18, pp. 17858–17870, Sep. 2022.

[15] Y. Almadani et al., "Visible light communications for industrial applications—Challenges and potentials," *Electronics*, vol. 9, no. 12, p. 2157, Dec. 2020.

[16] I. M. Abou-Shehada, A. F. AlMuallim, A. K. AlFaqeh, A. H. Muqaibel, K.-H. Park, and M.-S. Alouini, "Accurate indoor visible light positioning using a modified Pathloss model with sparse fingerprints," *J. Lightw. Technol.*, vol. 39, no. 20, pp. 6487–6497, Oct. 2021.

[17] T. Q. Wang, Y. A. Sekercioglu, A. Neild, and J. Armstrong, "Position accuracy of time-of-arrival based ranging using visible light with application in indoor localization systems," *J. Lightw. Technol.*, vol. 31, no. 20, pp. 3302–3308, Oct. 2013.

[18] Y. Zhuang et al., "A survey of positioning systems using visible LED lights," *IEEE Commun. Surveys Tuts.*, vol. 20, no. 3, pp. 1963–1988, 3rd Quart., 2018.

[19] M. Afzalan and F. Jazizadeh, "Indoor positioning based on visible light communication: A performance-based survey of real-world prototypes," *ACM Comput. Surveys*, vol. 52, no. 2, pp. 1–36, May 2019.

[20] M. Maheepala, A. Z. Kouzani, and M. A. Joordens, "Light-based indoor positioning systems: A review," *IEEE Sensors J.*, vol. 20, no. 8, pp. 3971–3995, Apr. 2020.

[21] H. Q. Tran and C. Ha, "Machine learning in indoor visible light positioning systems: A review," *Neurocomputing*, vol. 491, pp. 117–131, Jun. 2022.

[22] S. M. Sheikh, H. M. Asif, K. Raahemifar, and F. Al-Turjman, "Time difference of arrival based indoor positioning system using visible light communication," *IEEE Access*, vol. 9, pp. 52113–52124, 2021.

[23] A. Norrdine, "An algebraic solution to the multilateration problem," in *Proc. 15th Int. Conf. Indoor Position. Indoor Navigat.*, vol. 1315, 2012, pp. 1–5.

[24] J. Luo, L. Fan, and H. Li, "Indoor positioning systems based on visible light communication: State of the art," *IEEE Commun. Surveys Tuts.*, vol. 19, no. 4, pp. 2871–2893, 4th Quart., 2017.

[25] P. Du et al., "Experimental demonstration of 3D visible light positioning using received signal strength with low-complexity trilateration assisted by deep learning technique," *IEEE Access*, vol. 7, pp. 93986–93997, 2019.

[26] N. Chaudhary, L. N. Alves, and Z. Ghassemblooy, "Current trends on visible light positioning techniques," in *Proc. 2nd West Asian Colloq. Opt. Wireless Commun. (WACOWC)*, 2019, pp. 100–105.

[27] M. T. Zia, "Visible light communication based indoor positioning system," *TEM J.*, vol. 9, no. 1, pp. 30–36, 2020.

[28] B. Zhu, Z. Zhang, J. Dang, L. Wu, and L. Wang, "Low-complexity visible light positioning and rotation estimation based on eigenvalue decomposition," *J. Lightw. Technol.*, vol. 40, no. 21, pp. 7072–7083, Nov. 2022.

[29] B. Zhu, J. Cheng, Y. Wang, J. Yan, and J. Wang, "Three-dimensional VLC positioning based on angle difference of arrival with arbitrary tilting angle of receiver," *IEEE J. Sel. Areas Commun.*, vol. 36, no. 1, pp. 8–22, Jan. 2018.

[30] S. Shen, S. Li, and H. Steendam, "Simultaneous position and orientation estimation for visible light systems with multiple LEDs and multiple PDs," *IEEE J. Sel. Areas Commun.*, vol. 38, no. 8, pp. 1866–1879, Aug. 2020.

[31] S. Shen, S. Li, and H. Steendam, "Hybrid position and orientation estimation for visible light systems in the presence of prior information on the orientation," *IEEE Trans. Wireless Commun.*, vol. 21, no. 8, pp. 6271–6284, Aug. 2022.

[32] T. Komine and M. Nakagawa, "Fundamental analysis for visible-light communication system using LED lights," *IEEE Trans. Consum. Electron.*, vol. 50, no. 1, pp. 100–107, Feb. 2004.

[33] B. Turan, E. Kar, and S. Coleri, "Vehicular visible light communications noise analysis and Autoencoder based denoising," in *Proc. Joint Eur. Conf. Netw. Commun. 6G Summit (EuCNC/6G Summit)*, 2022, pp. 19–24.

[34] K. Zhang, Z. Zhang, and B. Zhu, "Beacon LED coordinates estimator for easy deployment of visible light positioning systems," *IEEE Trans. Wireless Commun.*, vol. 21, no. 12, pp. 10208–10223, Dec. 2022.

[35] Q. Liang, Y. Sun, C. Liu, M. Liu, and L. Wang, "LedMapper: Toward efficient and accurate LED mapping for visible light positioning at scale," *IEEE Trans. Instrum. Meas.*, vol. 71, pp. 1–12, 2022.

[36] R. Amsters, E. Demeester, P. Slaets, D. Holm, J. Joly, and N. Stevens, "Towards automated calibration of visible light positioning systems," in *Proc. Int. Conf. Indoor Position. Indoor Navigat. (IPIN)*, 2019, pp. 1–8.

[37] X. Guo, S. Shao, N. Ansari, and A. Khreishah, "Indoor localization using visible light via fusion of multiple classifiers," *IEEE Photon. J.*, vol. 9, no. 6, Dec. 2017, Art. no. 7803716.

[38] C.-W. Hsu, S. Liu, F. Lu, C.-W. Chow, C.-H. Yeh, and G.-K. Chang, "Accurate indoor visible light positioning system utilizing machine learning technique with height tolerance," in *Proc. Opt. Fiber Commun. Conf. Expo. (OFC)*, 2018, pp. 1–3.

[39] M. Saadi, Z. Saeed, T. Ahmad, M. K. Saleem, and L. Wuttisittikulkij, "Visible light-based indoor localization using k-means clustering and linear regression," *Trans. Emerg. Telecommun. Technol.*, vol. 30, no. 2, 2019, Art. no. e3480.

[40] F. Alam, M. T. Chew, T. Wenge, and G. S. Gupta, "An accurate visible light positioning system using regenerated fingerprint database based on calibrated propagation model," *IEEE Trans. Instrum. Meas.*, vol. 68, no. 8, pp. 2714–2723, Aug. 2019.

[41] M. Irshad, W. Liu, L. Wang, and M. U. R. Khalil, "Cogent machine learning algorithm for indoor and underwater localization using visible light spectrum," *Wireless Pers. Commun.*, vol. 116, no. 2, pp. 993–1008, Jan. 2021.

[42] H. Q. Tran and C. Ha, "Fingerprint-based indoor positioning system using visible light communication—A novel method for multipath reflections," *Electronics*, vol. 8, no. 1, p. 63, Jan. 2019.

[43] H. Tran and C. Ha, "Improved visible light-based indoor positioning system using machine learning classification and regression," *Appl. Sci.*, vol. 9, no. 6, p. 1048, Mar. 2019.

[44] J. Jiang, W. Guan, Z. Chen, and Y. Chen, "Indoor high-precision three-dimensional positioning algorithm based on visible light communication and fingerprinting using K-means and random forest," *Opt. Eng.*, vol. 58, p. 1, Jan. 2019.

[45] X. Guo, F. Hu, N. R. Elikplim, and L. Li, "Indoor localization using visible light via two-layer fusion network," *IEEE Access*, vol. 7, pp. 16421–16430, 2019.

[46] M. Saadi, T. Ahmad, Y. Zhao, and L. Wuttisttikulkij, "An LED based indoor localization system using k-means clustering," in *Proc. 15th IEEE Int. Conf. Mach. Learn. Appl. (ICMLA)*, 2016, pp. 246–252.

[47] A. Gradim, P. Fonseca, L. N. Alves, and R. E. Mohamed, "On the usage of machine learning techniques to improve position accuracy in visible light positioning systems," in *Proc. 11th Int. Symp. Commun. Syst., Netw. Digit. Signal Process. (CSNDSP)*, 2018, pp. 1–6.

[48] Y.-C. Chuang, Z.-Q. Li, C.-W. Hsu, Y. Liu, and C.-W. Chow, "Visible light communication and positioning using positioning cells and machine learning algorithms," *Opt. Exp.*, vol. 27, no. 11, pp. 16377–16383, May 2019.

[49] Z. Yuan, X. Zha, and X. Zhang, "Adaptive multi-type fingerprint indoor positioning and Localization method based on multi-task learning and weight coefficients K-nearest Neighbor," *Sensors*, vol. 20, no. 18, p. 5416, Sep. 2020.

[50] C.-Y. Hong et al., "Angle-of-arrival (AOA) visible light positioning (VLP) system using solar cells with third-order regression and ridge regression algorithms," *IEEE Photon. J.*, vol. 12, no. 3, Jun. 2020, Art. no. 7902605.

[51] W. Raes, N. Knudde, J. De Bruycker, T. Dhaene, and N. Stevens, "Experimental evaluation of machine learning methods for robust received signal strength-based visible light positioning," *Sensors*, vol. 20, no. 21, p. 6109, Oct. 2020.

[52] H. Q. Tran and C. Ha, "High precision weighted optimum K-nearest neighbors algorithm for indoor visible light positioning applications," *IEEE Access*, vol. 8, pp. 114597–114607, 2020.

[53] C.-Y. Hong et al., "Using silicon photovoltaic cells and machine learning and neural network algorithms for visible-light positioning systems," *Opt. Eng.*, vol. 59, no. 9, 2020, Art. no. 96107.

[54] N. Faulkner, F. Alam, M. Legg, and S. Demidenko, "Watchers on the wall: Passive visible light-based positioning and tracking with embedded light-sensors on the wall," *IEEE Trans. Instrum. Meas.*, vol. 69, no. 5, pp. 2522–2532, May 2020.

[55] A. H. Abu Bakar, T. Glass, H. Y. Tee, F. Alam, and M. Legg, "Accurate visible light positioning using multiple-photodiode receiver and machine learning," *IEEE Trans. Instrum. Meas.*, vol. 70, 2021, Art. no. 7500812.

[56] S.-H. Song et al., "Employing DIALux to relieve machine-learning training data collection when designing indoor positioning systems," *Opt. Exp.*, vol. 29, no. 11, pp. 16887–16892, May 2021.

[57] H. Chen et al., "High accuracy indoor visible light positioning using a long short term memory-fully connected network based algorithm," *Opt. Exp.*, vol. 29, no. 25, pp. 41109–41120, Dec. 2021.

[58] H. Q. Tran and C. Ha, "Reducing the burden of data collection in a fingerprinting-based VLP system using a hybrid of improved co-training semi-supervised regression and adaptive boosting algorithms," *Opt. Commun.*, vol. 488, Jun. 2021, Art. no. 126857.

[59] E. Aparicio-Esteve, W. Raes, N. Stevens, J. Ureña, and Á. Hernández, "Experimental evaluation of a machine learning-based RSS localization method using Gaussian processes and a quadrant photodiode," *J. Lightw. Technol.*, vol. 40, no. 19, pp. 6388–6396, Oct. 2022.

[60] R. Liu, Z. Liang, K. Yang, and W. Li, "Machine learning based visible light indoor positioning with single-LED and single rotatable photo detector," *IEEE Photon. J.*, vol. 14, no. 3, pp. 1–11, Jun. 2022.

[61] F. Che et al., "Feature-based generalized Gaussian distribution method for NLoS detection in ultra-wideband (UWB) indoor positioning system," *IEEE Sensors J.*, vol. 22, no. 19, pp. 18726–18739, Oct. 2022.

[62] A. M. Abdalmajeed, M. Mahmoud, A. E.-R. A. El-Fikky, H. A. Fayed, and M. H. Aly, "Improved indoor visible light positioning system using machine learning," *Opt. Quant. Electron.*, vol. 55, no. 3, p. 209, 2023.

[63] Y. Chen, W. Guan, J. Li, and H. Song, "Indoor real-time 3-D visible light positioning system using fingerprinting and extreme learning machine," *IEEE Access*, vol. 8, pp. 13875–13886, 2020.

[64] Z. Zhang, Y. Zhu, W. Zhu, H. Chen, X. Hong, and J. Chen, "Iterative point-wise reinforcement learning for highly accurate indoor visible light positioning," *Opt. Exp.*, vol. 27, no. 16, pp. 22161–22172, Aug. 2019.

[65] Z. Zhang, H. Chen, W. Zeng, X. Cao, X. Hong, and J. Chen, "Demonstration of three-dimensional indoor visible light positioning with multiple photodiodes and reinforcement learning," *Sensors*, vol. 20, no. 22, p. 6470, Nov. 2020.

[66] B. Zhang, D. Han, M. Zhang, L. Wang, and X. Li, "Reinforcement learning-based visible light positioning and handover scheme with stereo-camera," *IEEE Access*, vol. 10, pp. 76512–76522, 2022.

[67] X. Li, Y. Cao, and C. Chen, "Machine learning based high accuracy indoor visible light location algorithm," in *Proc. IEEE Int. Conf. Smart Internet Things (SmartIoT)*, 2018, pp. 198–203.

[68] T. Yuan, Y. Xu, Y. Wang, P. Han, and J. Chen, "A tilt receiver correction method for visible light positioning using machine learning method," *IEEE Photon. J.*, vol. 10, no. 6, Dec. 2018, Art. no. 7909312.

[69] I. Alonso-González, D. Sánchez-Rodríguez, C. Ley-Bosch, and M. Quintana-Suárez, "Discrete indoor three-dimensional localization system based on neural networks using visible light communication," *Sensors*, vol. 18, no. 4, p. 1040, Mar. 2018.

[70] Z. Wang et al., "Deep convolutional auto-encoder based indoor light positioning using RSS temporal image," in *Proc. IEEE Int. Symp. Broadband Multimedia Syst. Broadcast. (BMSB)*, 2019, pp. 1–5.

[71] J. He et al., "Demonstration of high precision 3D indoor positioning system based on two-layer ANN machine learning technique," in *Proc. Opt. Fiber Commun. Conf. Exhibit. (OFC)*, 2019, pp. 1–3.

[72] H. Zhang et al., "High-precision indoor visible light positioning using modified momentum back propagation neural network with sparse training point," *Sensors*, vol. 19, no. 10, p. 2324, May 2019.

[73] H. Zhang et al., "High-precision indoor visible light positioning using deep neural network based on the Bayesian regularization with sparse training point," *IEEE Photon. J.*, vol. 11, no. 3, Jun. 2019, Art. no. 7903310.

[74] S. Zhang, P. Du, C. Chen, W.-D. Zhong, and A. Alphones, "Robust 3D indoor VLP system based on ANN using hybrid RSS/PDOA," *IEEE Access*, vol. 7, pp. 47769–47780, 2019.

[75] S. Ni et al., "An indoor visible light communication and positioning system based on machine learning and Alamouti STBC," in *Proc. Conf. Lasers Electro-Opt.*, 2020, p. SW4L.1.

[76] X. Wang, Z. Yu, and S. Mao, "Indoor localization using smartphone magnetic and light sensors: A deep LSTM approach," *Mobile Netw. Appl.*, vol. 25, pp. 819–832, Apr. 2020.

[77] X. Lin and L. Zhang, "Intelligent and practical deep learning aided positioning design for visible light communication receivers," *IEEE Commun. Lett.*, vol. 24, no. 3, pp. 577–580, Mar. 2020.

[78] A. A. Mahmoud, Z. U. Ahmad, O. C. Haas, and S. Rajbhandari, "Precision indoor three-dimensional visible light positioning using receiver diversity and multi-layer perceptron neural network," *IET Optoelectron.*, vol. 14, no. 6, pp. 440–446, 2020.

[79] W. Raes, J. De Bruycker, and N. Stevens, "A cellular approach for large scale, machine learning based visible light positioning solutions," in *Proc. Int. Conf. Indoor Position. Indoor Navigat. (IPIN)*, 2021, pp. 1–6.

[80] L. Hua, Y. Zhuang, F. Gu, L. Qi, and J. Yang, "AdVLP: Unsupervised visible light positioning by adversarial deep learning," *Meas. Sci. Technol.*, vol. 32, no. 6, 2021, Art. no. 64003.

[81] X. Li, D. Han, S. Zhao, Q. Li, and M. Zhang, "Artificial neural network-embedded millimeter-level 3D positioning system with single LED and monitoring camera," *Opt. Eng.*, vol. 60, no. 7, pp. 076103–076103, 2021.

[82] Z. Cao, M. Cheng, Q. Yang, M. Tang, D. Liu, and L. Deng, "Experimental investigation of environmental interference mitigation and blocked LEDs using a memory-artificial neural network in 3D indoor visible light positioning systems," *Opt. Exp.*, vol. 29, no. 21, pp. 33937–33953, 2021.

[83] M. A. Arfaoui et al., "Invoking deep learning for joint estimation of indoor LiFi user position and orientation," *IEEE J. Sel. Areas Commun.*, vol. 39, no. 9, pp. 2890–2905, Sep. 2021.

[84] K. Majeed and S. Hranilovic, "Passive indoor visible light positioning system using deep learning," *IEEE Internet Things J.*, vol. 8, no. 19, pp. 14810–14821, Oct. 2021.

[85] D.-C. Lin et al., "Positioning unit cell model duplication with residual concatenation neural network (RCNN) and transfer learning for visible light positioning (VLP)," *J. Lightw. Technol.*, vol. 39, no. 20, pp. 6366–6372, Oct. 2021.

[86] L. Zhao, J. Chen, and H. Liu, "Neural network visible light indoor location based on lambert model optimization," in *Proc. IEEE 10th Int. Conf. Inf. Commun. Netw. (ICICN)*, 2022, pp. 202–207.

[87] L.-S. Hsu, C.-W. Chow, Y. Liu, and C.-H. Yeh, "3D visible light-based indoor positioning system using two-stage neural network (TSNN) and received intensity selective enhancement (RISE) to alleviate light non-overlap zones," *Sensors*, vol. 22, no. 22, p. 8817, 2022.

[88] N. Chaudhary, O. I. Younus, L. N. Alves, Z. Ghassemlooy, and S. Zvanovec, "The usage of ANN for regression analysis in visible light positioning systems," *Sensors*, vol. 22, no. 8, p. 2879, 2022.

[89] L.-S. Hsu et al., "Using data pre-processing and convolutional neural network (CNN) to mitigate light deficient regions in visible light positioning (VLP) systems," *J. Lightw. Technol.*, vol. 40, no. 17, pp. 5894–5900, Sep. 2022.

[90] L.-S. Hsu et al., "Utilizing single light-emitting-diode (LED) lamp and silicon solar-cells visible light positioning (VLP) based on angle-of-arrival (AOA) and long-short-term-memory-neural-network (LSTMNN)," *Opt. Commun.*, vol. 524, Dec. 2022, Art. no. 128761.

[91] X.-B. Wu, S.-S. Wen, and J. Hua, "High precision 3D positioning system design using visible light communication based on ant colony algorithm," *Acta Photonica Sinica*, vol. 46, no. 12, 2017, Art. no. 1206004.

[92] W. Guan, Y. Wu, C. Xie, H. Chen, Y. Cai, and Y. Chen, "High-precision approach to localization scheme of visible light communication based on artificial neural networks and modified genetic algorithms," *Opt. Eng.*, vol. 56, no. 10, 2017, Art. no. 106103.

[93] Y. Cai, W. Guan, Y. Wu, C. Xie, Y. Chen, and L. Fang, "Indoor high precision three-dimensional positioning system based on visible light communication using particle swarm optimization," *IEEE Photon. J.*, vol. 9, no. 6, Dec. 2017, Art. no. 7908120.

[94] M. Zhang et al., "A three-dimensional indoor positioning technique based on visible light communication using chaotic particle swarm optimization algorithm," *Optik*, vol. 165, pp. 54–73, Jul. 2018.

[95] Y. Wu, Y. Xian, W. Guan, X. Chen, Q. Peng, and B. Chen, "High-precision indoor three-dimensional localization scheme based on visible light communication using modified fruit fly optimization algorithm," *Opt. Eng.*, vol. 57, no. 6, pp. 66115–66115, 2018.

[96] S. Wen, X. Cai, W. Guan, J. Jiang, B. Chen, and M. Huang, "High-precision indoor three-dimensional positioning system based on visible light communication using modified artificial fish swarm algorithm," *Opt. Eng.*, vol. 57, no. 10, 2018, Art. no. 106102.

[97] Y. Wu, X. Liu, W. Guan, B. Chen, X. Chen, and C. Xie, "High-speed 3D indoor localization system based on visible light communication using differential evolution algorithm," *Opt. Commun.*, vol. 424, pp. 177–189, Oct. 2018.

[98] H. Chen, W. Guan, S. Li, and Y. Wu, "Indoor high precision three-dimensional positioning system based on visible light communication using modified genetic algorithm," *Opt. Commun.*, vol. 413, pp. 103–120, Apr. 2018.

[99] B. Zhou, V. Lau, Q. Chen, and Y. Cao, "Simultaneous positioning and orientating for visible light communications: Algorithm design and performance analysis," *IEEE Trans. Veh. Technol.*, vol. 67, no. 12, pp. 11790–11804, Dec. 2018.

[100] Q. Peng, W. Guan, Y. Wu, Y. Cai, C. Xie, and P. Wang, "Three-dimensional high-precision indoor positioning strategy using tabu search based on visible light communication," *Opt. Eng.*, vol. 57, no. 1, 2018, Art. no. 16101.

[101] Á. De-La-Llana-Calvo, J. Lázaro-Galilea, A. Gardel-Vicente, D. Rodríguez-Navarro, and I. Bravo-Muñoz, "Indoor positioning system based on LED lighting and PSD sensor," in *Proc. Int. Conf. Indoor Position. Indoor Navigat. (IPIN)*, 2019, pp. 1–8.

[102] G. Pau, M. Collotta, V. Maniscalco, and K.-K. R. Choo, "A fuzzy-PSO system for indoor localization based on visible light communications," *Soft Comput.*, vol. 23, pp. 5547–5557, Jul. 2019.

[103] L. Huang, P. Wang, Z. Liu, X. Nan, L. Jiao, and L. Guo, "Indoor three-dimensional high-precision positioning system with bat algorithm based on visible light communication," *Appl. Opt.*, vol. 58, no. 9, pp. 2226–2234, 2019.

[104] C. Carreño et al., "Comparison of metaheuristic optimization algorithms for RSS-based 3-D visible light positioning systems," in *Proc. South Amer. Colloq. Visible Light Commun. (SACVC)*, 2020, pp. 1–6.

[105] S. Xu, Y. Wu, X. Wang, and F. Wei, "Indoor 3D visible light positioning system based on adaptive parameter particle swarm optimisation," *IET Commun.*, vol. 14, no. 20, pp. 3707–3714, 2020.

[106] Y. Chen, H. Zheng, H. Liu, Z. Han, and Z. Ren, "Indoor high precision three-dimensional positioning system based on visible light communication using improved hybrid bat algorithm," *IEEE Photon. J.*, vol. 12, no. 5, Oct. 2020, Art. no. 6802513.

[107] J. Dang, S. Gao, Z. Zhang, L. Wu, B. Zhu, and L. Wang, "Joint optimization for visible light communication and positioning based on information entropy," in *Proc. 7th Int. Conf. Comput. Commun. (ICCC)*, 2021, pp. 403–409.

[108] Y. Huang, X. Zhang, E.-H. Aglzim, and L. Shi, "Target 5G visible light positioning signal subcarrier extraction method using particle swarm optimization algorithm," in *Proc. IEEE Int. Symp. Broadband Multimedia Syst. Broadcast. (BMSB)*, 2021, pp. 1–6.

[109] Y. Chen, Z. Ren, Z. Han, H. Liu, Q.-X. Shen, and Z. Wu, "LED based high accuracy indoor visible light positioning algorithm," *Optik*, vol. 243, Oct. 2021, Art. no. 166853.

[110] H. Zhao, W. Njima, X. Zhang, and F. Bader, "High resolution visible-light localization in industrial dynamic environment: A robustness approach based on the PSO algorithm," in *Proc. IEEE 12th Int. Conf. Indoor Position. Indoor Navigat. (IPIN)*, 2022, pp. 1–8.

[111] J. Chaochuan, Y. Ting, W. Chuanjiang, and S. Mengli, "High-accuracy 3D indoor visible light positioning method based on the improved adaptive cuckoo search algorithm," *Arabian J. Sci. Eng.*, vol. 47, no. 2, pp. 2479–2498, 2022.

[112] X. Meng, C. Jia, C. Cai, F. He, and Q. Wang, "Indoor high-precision 3D positioning system based on visible-light communication using improved whale optimization algorithm," *Photonics*, vol. 9, no. 2, p. 93, 2022.

[113] Z. Wang, Z. Liang, X. Li, and H. Li, "Indoor visible light positioning based on improved particle swarm optimization method with min-max algorithm," *IEEE Access*, vol. 10, pp. 130068–130077, 2022.

[114] Q. Wu, J. Zhang, and J.-N. Guo, "Position design for reconfigurable intelligent-surface-aided indoor visible light communication systems," *Electronics*, vol. 11, no. 19, p. 3076, Sep. 2022.

[115] W. Costa et al., "Toward AI-enhanced VLC systems for industrial applications," *J. Lightw. Technol.*, vol. 41, no. 4, pp. 1064–1076, Feb. 2023.

[116] J. Lin et al., "Using four-quadrant photodetector and improved genetic algorithm for visible-light positioning system," *Opt. Eng.*, vol. 61, no. 4, 2022, Art. no. 44107.

[117] Á. De-La-Llana-Calvo et al., "Weak calibration of a visible light positioning system based on a position-sensitive detector: Positioning error assessment," *Sensors*, vol. 21, no. 11, p. 3924, Jun. 2021.

[118] F. Wei, Y. Wu, S. Xu, and X. Wang, "Accurate visible light positioning technique using extreme learning machine and meta-heuristic algorithm," *Opt. Commun.*, vol. 532, Apr. 2023, Art. no. 129245.

[119] V. N. Saxena, V. K. Dwivedi, and J. Gupta, "Machine learning in visible light communication system: A survey," *Wireless Commun. Mobile Comput.*, vol. 2023, Feb. 2023, Art. no. 3950657.

[120] S. M. Sheikholeslami, A. Rasti-Meymandi, S. J. Seyed-Mohammadi, J. Abouei, and K. N. Plataniotis, "Communication-efficient federated learning for hybrid VLC/RF indoor systems," *IEEE Access*, vol. 10, pp. 126479–126493, 2022.

[121] B. A. Salau, A. Rawal, and D. B. Rawat, "Recent advances in artificial intelligence for wireless Internet of Things and Cyber–physical systems: A comprehensive survey," *IEEE Internet Things J.*, vol. 9, no. 15, pp. 12916–12930, Aug. 2022.

[122] M. M. Hossain Shuvo, S. K. Islam, J. Cheng, and B. I. Morshed, "Efficient acceleration of deep learning inference on resource-constrained edge devices: A review," *Proc. IEEE*, vol. 111, no. 1, pp. 42–91, Jan. 2023.

[123] Z. Jan et al., "Artificial intelligence for industry 4.0: Systematic review of applications, challenges, and opportunities," *Exp. Syst. Appl.*, vol. 216, Apr. 2023, Art. no. 119456.

[124] M. S. Mollel et al., "A survey of machine learning applications to handover management in 5G and beyond," *IEEE Access*, vol. 9, pp. 45770–45802, 2021.

[125] F. de Oliveira Torres, V. A. de Santiago Júnior, D. B. da Costa, D. L. Cardoso, and R. C. L. de Oliveira, "Throughput maximization for a multicarrier cell-less NOMA network: A framework based on ensemble metaheuristics," *IEEE Trans. Wireless Commun.*, vol. 22, no. 1, pp. 348–361, Jan. 2023.

[126] V. Sharma and A. K. Tripathi, "A systematic review of meta-heuristic algorithms in IoT based application," *Array*, vol. 14, Jul. 2022, Art. no. 100164.

[127] R. P. Parouha and P. Verma, "State-of-the-art reviews of meta-heuristic algorithms with their novel proposal for unconstrained optimization and applications," *Arch. Comput. Methods Eng.*, vol. 28, pp. 4049–4115, Aug. 2021.

[128] A. X. Wang, S. S. Chukova, and B. P. Nguyen, "Ensemble k-nearest neighbors based on centroid displacement," *Inf. Sci.*, vol. 629, pp. 313–323, Jun. 2023.

[129] H. Zhang, B. Quost, and M.-H. Masson, "Cautious weighted random forests," *Exp. Syst. Appl.*, vol. 213, Mar. 2023, p. 118883.

[130] K. P. Sinaga and M.-S. Yang, "Unsupervised K-means clustering algorithm," *IEEE Access*, vol. 8, pp. 80716–80727, 2020.

[131] Y. Chen et al., "KNN-BLOCK DBSCAN: Fast clustering for large-scale data," *IEEE Trans. Syst., Man, Cybern., Syst.*, vol. 51, no. 6, pp. 3939–3953, Jun. 2021.

[132] H. H. Kenchannavar, P. M. Pujar, R. M. Kulkarni, and U. P. Kulkarni, "Evaluation and analysis of goodness of fit for water quality parameters using linear regression through the Internet-of-Things-based water quality monitoring system," *IEEE Internet Things J.*, vol. 9, no. 16, pp. 14400–14407, Aug. 2022.

[133] C.-H. Yu, F. Gao, and Q.-Y. Wen, "An improved quantum algorithm for ridge regression," *IEEE Trans. Knowl. Data Eng.*, vol. 33, no. 3, pp. 858–866, Mar. 2021.

[134] J. Choi, "Data-aided sensing for Gaussian process regression in IoT systems," *IEEE Internet Things J.*, vol. 8, no. 9, pp. 7717–7726, May 2021.

[135] F. Zhu, J. Gao, C. Xu, J. Yang, and D. Tao, "On selecting effective patterns for fast support vector regression training," *IEEE Trans. Neural Netw. Learn. Syst.*, vol. 29, no. 8, pp. 3610–3622, Aug. 2018.

[136] J. Cao, K. Zhang, H. Yong, X. Lai, B. Chen, and Z. Lin, "Extreme learning machine with affine transformation inputs in an activation function," *IEEE Trans. Neural Netw. Learn. Syst.*, vol. 30, no. 7, pp. 2093–2107, Jul. 2019.

[137] M. Chen, U. Challita, W. Saad, C. Yin, and M. Debbah, "Artificial neural networks-based machine learning for wireless networks: A tutorial," *IEEE Commun. Surveys Tuts.*, vol. 21, no. 4, pp. 3039–3071, 4th Quart., 2019.

[138] M. A. Al-Garadi, A. Mohamed, A. K. Al-Ali, X. Du, I. Ali, and M. Guizani, "A survey of machine and deep learning methods for Internet of Things (IoT) security," *IEEE Commun. Surveys Tuts.*, vol. 22, no. 3, pp. 1646–1685, 3rd Quart., 2020.

[139] L. Xing and W. Liu, "A data fusion powered bi-directional long short term memory model for predicting multi-lane short term traffic flow," *IEEE Trans. Intell. Transp. Syst.*, vol. 23, no. 9, pp. 16810–16819, Sep. 2022.

[140] D. A. Tubiana, J. Farhat, G. Brante, and R. D. Souza, "Q-learning NOMA random access for IoT-satellite terrestrial relay networks," *IEEE Wireless Commun. Lett.*, vol. 11, no. 8, pp. 1619–1623, Aug. 2022.

[141] M. Nasr-Azadani, J. Abouei, and K. N. Plataniotis, "Single- and multiagent actor–critic for initial UAV's deployment and 3-D trajectory design," *IEEE Internet Things J.*, vol. 9, no. 16, pp. 15372–15389, Aug. 2022.

[142] D. Charte, F. Charte, S. García, M. J. del Jesus, and F. Herrera, "A practical tutorial on autoencoders for nonlinear feature fusion: Taxonomy, models, software and guidelines," *Inf. Fusion*, vol. 44, pp. 78–96, Nov. 2018.

[143] T. Kotsiopoulos, P. Sarigiannidis, D. Ioannidis, and D. Tzovaras, "Machine learning and deep learning in smart manufacturing: The smart grid paradigm," *Comput. Sci. Rev.*, vol. 40, May 2021, Art. no. 100341.

[144] G. Shanmugasundar, M. Vanitha, R. Čep, V. Kumar, K. Kalita, and M. Ramachandran, "A comparative study of linear, random forest and AdaBoost regressions for modeling non-traditional machining," *Processes*, vol. 9, no. 11, p. 2015, Nov. 2021.

[145] M. E. Celebi, H. A. Kingravi, and P. A. Vela, "A comparative study of efficient initialization methods for the k-means clustering algorithm," *Exp. Syst. Appl.*, vol. 40, no. 1, pp. 200–210, 2013.

[146] A. E. Ezugwu et al., "A comprehensive survey of clustering algorithms: State-of-the-art machine learning applications, taxonomy, challenges, and future research prospects," *Eng. Appl. Artif. Intell.*, vol. 110, Apr. 2022, Art. no. 104743.

[147] D. Xu and Y. Tian, "A comprehensive survey of clustering algorithms," *Ann. Data Sci.*, vol. 2, pp. 165–193, Jun. 2015.

[148] M. G. M. Abdolrasol et al., "Artificial neural networks based optimization techniques: A review," *Electronics*, vol. 10, no. 21, Nov. 2021, Art. no. 2689.

[149] F. Perez-Cruz, S. Van Vaerenbergh, J. J. Murillo-Fuentes, M. Lazaro-Gredilla, and I. Santamaria, "Gaussian processes for nonlinear signal processing: An overview of recent advances," *IEEE Signal Process. Mag.*, vol. 30, no. 4, pp. 40–50, Jul. 2013.

[150] K. Jakkala, "Deep Gaussian processes: A survey," 2021, *arXiv:2106.12135*.

[151] J. Wang, S. Lu, S.-H. Wang, and Y.-D. Zhang, "A review on extreme learning machine," *Multimedia Tools Appl.*, vol. 81, no. 29, pp. 41611–41660, 2022.

[152] Y. Wang, F. Cao, and Y. Yuan, "A study on effectiveness of extreme learning machine," *Neurocomputing*, vol. 74, no. 16, pp. 2483–2490, 2011.

[153] E. J. Bredensteiner and K. P. Bennett, "Multicategory classification by support vector machines," *Comput. Optim. Appl.*, vol. 12, pp. 53–79, sep. 1999.

[154] Y. Keneshloo, T. Shi, N. Ramakrishnan, and C. K. Reddy, "Deep reinforcement learning for sequence-to-sequence models," *IEEE Trans. Neural Netw. Learn. Syst.*, vol. 31, no. 7, pp. 2469–2489, Jul. 2020.

[155] T. T. Nguyen, N. D. Nguyen, and S. Nahavandi, "Deep reinforcement learning for multiagent systems: A review of challenges, solutions, and applications," *IEEE Trans. Cybern.*, vol. 50, no. 9, pp. 3826–3839, Sep. 2020.

[156] H. M. Abdullah, A. Gastli, and L. Ben-Brahim, "Reinforcement learning based EV charging management systems—A review," *IEEE Access*, vol. 9, pp. 41506–41531, 2021.

[157] T. Harada and E. Alba, "Parallel genetic algorithms: A useful survey," *ACM Comput. Surveys*, vol. 53, no. 4, pp. 1–39, Aug. 2020.

[158] A. Krohn, S. Pachnicke, and P. A. Hoeher, "Genetic optimization of liquid crystal matrix based interference suppression for VLC MIMO transmissions," *IEEE Photon. J.*, vol. 14, no. 1, Feb. 2022, Art. no. 7300705.

[159] J. Nayak, H. Swapnarekha, B. Naik, G. Dhiman, and S. Vimal, "25 years of particle swarm optimization: Flourishing voyage of two decades," *Arch. Comput. Methods Eng.*, vol. 30, pp. 1663–1725, Apr. 2023.

[160] S. K. Goudos, *Emerging Evolutionary Algorithms for Antennas and Wireless Communications*. London, U.K.: IET, 2021.

[161] S. Bastiaens, S. K. Goudos, W. Joseph, and D. Plets, "Metaheuristic optimization of LED locations for visible light positioning network planning," *IEEE Trans. Broadcast.*, vol. 67, no. 4, pp. 894–908, Dec. 2021.

[162] Y. del Valle, G. K. Venayagamoorthy, S. Mohagheghi, J.-C. Hernandez, and R. G. Harley, "Particle swarm optimization: Basic concepts, variants and applications in power systems," *IEEE Trans. Evol. Comput.*, vol. 12, no. 2, pp. 171–195, Apr. 2008.

[163] M. R. AlRashidi and M. E. El-Hawary, "A survey of particle swarm optimization applications in electric power systems," *IEEE Trans. Evol. Comput.*, vol. 13, no. 4, pp. 913–918, Aug. 2009.

[164] W. Deng et al., "An enhanced fast non-dominated solution sorting genetic algorithm for multi-objective problems," *Inf. Sci.*, vol. 585, pp. 441–453, Mar. 2022.

[165] A. Younis, A. Bakhit, M. Onsa, and M. Hashim, "A comprehensive and critical review of bio-inspired metaheuristic frameworks for extracting parameters of solar cell single and double diode models," *Energy Rep.*, vol. 8, pp. 7085–7106, Nov. 2022.

[166] M. F. Ahmad, N. A. M. Isa, W. H. Lim, and K. M. Ang, "Differential evolution: A recent review based on state-of-the-art works," *Alexandria Eng. J.*, vol. 61, no. 5, pp. 3831–3872, 2022.

[167] S. Das and P. N. Suganthan, "Differential evolution: A survey of the state-of-the-art," *IEEE Trans. Evol. Comput.*, vol. 15, no. 1, pp. 4–31, Feb. 2011.

[168] T. Agarwal and V. Kumar, "A systematic review on bat algorithm: Theoretical foundation, variants, and applications," *Arch. Comput. Methods Eng.*, vol. 29, pp. 2707–2736, Aug. 2022.

[169] M. Shehab et al., "A comprehensive review of bat inspired algorithm: Variants, applications, and hybridization," *Arch. Comput. Methods Eng.*, vol. 30, no. 2, pp. 765–797, 2023.

[170] Y. Hou, H. Gao, Z. Wang, and C. Du, "Improved grey wolf optimization algorithm and application," *Sensors*, vol. 22, no. 10, p. 3810, May 2022.

[171] J. Liu, X. Wei, and H. Huang, "An improved grey wolf optimization algorithm and its application in path planning," *IEEE Access*, vol. 9, pp. 121944–121956, 2021.

[172] A. Nessa, B. Adhikari, F. Hussain, and X. N. Fernando, "A survey of machine learning for indoor positioning," *IEEE Access*, vol. 8, pp. 214945–214965, 2020.

[173] M. F. Keskin, A. D. Sezer, and S. Gezici, "Localization via visible light systems," *Proc. IEEE*, vol. 106, no. 6, pp. 1063–1088, Jun. 2018.

[174] B. Xie et al., "LIPS: A light intensity–based positioning system for indoor environments," *ACM Trans. Sensor Netw.*, vol. 12, no. 4, pp. 1–27, 2016.

[175] T.-H. Do and M. Yoo, "An in-depth survey of visible light communication based positioning systems," *Sensors*, vol. 16, no. 5, p. 678, May 2016.

[176] S. Bastiaens, M. Alijani, W. Joseph, and D. Plets, "An experimental analysis of visible light positioning in NLoS environments," in *Proc. IPIN*, Sep. 2023.

[177] S. S. Oyewobi, K. Djouani, and A. M. Kurien, "Visible light communications for Internet of Things: Prospects and approaches, challenges, solutions and future directions," *Technologies*, vol. 10, no. 1, p. 28, Feb. 2022.

[178] P. Chen, M. Pang, D. Che, Y. Yin, D. Hu, and S. Gao, "A survey on visible light positioning from software algorithms to hardware," *Wireless Commun. Mobile Comput.*, vol. 2021, pp. 1–20, Feb. 2021.

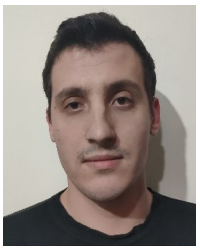

**VASILEIOS P. REKKAS** (Graduate Student Member, IEEE) received the B.Sc. degree in physics and the M.Sc. degree in electronic physics (radioelectrology) from the Aristotle University of Thessaloniki in 2017 and 2020, respectively, where he is currently pursuing the Ph.D. degree. His research interests lie in the areas of wireless communications, radio propagation, artificial intelligence techniques (machine learning, deep learning methods, and evolutionary algorithms), antenna design, and electromagnetics, while his Ph.D. research is funded by the Hellenic Foundation for Research and Innovation.

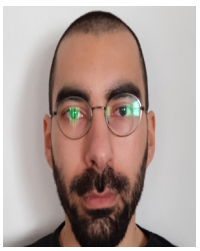

**LAZAROS ALEXIOS ILIADIS** (Graduate Student Member, IEEE) received the B.Sc. degree in physics and the M.Sc. degree in electronic physics (Radioelectrology) from the Aristotle University of Thessaloniki in 2017 and 2021, respectively, where he is currently pursuing the Ph.D. degree. His research interests include the development of the sixth-generation communications systems, antenna design and electromagnetics, artificial intelligence techniques (evolutionary algorithms, machine learning, and deep learning methods), and computer vision.

**SOTIRIOS P. SOTIROUDIS** received the first B.Sc. degree in physics, the M.Sc. degree in electronics, and the Ph.D. degree in physics from the Aristotle University of Thessaloniki in 1999, 2002, and 2018, respectively, and the second B.Sc. degree in informatics from Hellenic Open University in 2011. From 2004 to 2010, he worked with the Telecommunications Center, Aristotle University of Thessaloniki, while from 2010 to 2022, he worked with the Greek Ministry of Education as a Teacher of Physics and Informatics. He joined the Department of Physics, Aristotle University of Thessaloniki in 2022. He has been involved in several research projects. His research interests include wireless communications, radio propagation, optimization algorithms, computer vision, and machine learning.

**ACHILLES D. BOURSIANIS** (Member, IEEE) received the B.Sc. degree in physics, the M.Sc. degree in electronic physics (Radioelectrology) with expertise in electronics telecommunications technology, and the Ph.D. degree in telecommunications from the School of Physics, Aristotle University of Thessaloniki in 2001, 2005, and 2017, respectively.

From 2019 to 2023, he served as a Postdoctoral Researcher and an Academic Fellow with the School of Physics, Aristotle University of Thessaloniki, where he joined the School of Physics as a Laboratory Teaching Staff in 2023. He is also a member of the ELEDIA@AUTH Research Group. He is an author or coauthor of more than 70 articles in international peer-reviewed journals and conferences. His research interests include wireless sensor networks, Internet of Things, antenna design and optimization, 5G and beyond communication networks, radio frequency energy harvesting, and artificial intelligence.

Dr. Boursianis serves as a reviewer in several international journals and conferences and as a member of the technical program committee in various international conferences, which are technically sponsored by IEEE. He is a member of the editorial board of the *Telecom Journal*. He is a member of the Hellenic Physical Society, and the scientific committee of the National Association of Fédération des ingénieurs des télécommunications de la Communauté européenne (FITCE).

**PANAGIOTIS SARIGIANNIDIS** (Member, IEEE) received the B.Sc. and Ph.D. degrees in computer science from the Aristotle University of Thessaloniki, Thessaloniki, Greece, in 2001 and 2007, respectively. He is the Director of the ITHACA Lab, a Co-Founder of the first spin-off of the University of Western Macedonia, Kozani, Greece: MetaMind Innovations P.C., and an Associate Professor with the Department of Electrical and Computer Engineering, University of Western Macedonia. He has published over 330 papers in international journals, conferences and book chapters, including IEEE COMMUNICATIONS SURVEYS AND TUTORIALS, IEEE TRANSACTIONS ON COMMUNICATIONS, IEEE INTERNET OF THINGS, IEEE TRANSACTIONS ON BROADCASTING, IEEE SYSTEMS JOURNAL, *IEEE Wireless Communications Magazine*, IEEE OPEN JOURNAL OF THE COMMUNICATIONS SOCIETY, IEEE/OSA JOURNAL OF LIGHTWAVE TECHNOLOGY, IEEE TRANSACTIONS ON INDUSTRIAL INFORMATICS, IEEE ACCESS, and *Computer Networks*. His research interests include telecommunication networks, Internet of Things, and network security. He received six best paper awards and the IEEE SMC TCHS Research and Innovation Award 2023. He has been involved in several national, European, and international projects, coordinating four H2020/Horizon Europe projects, namely, DS-07-2017, SPEAR: Secure and Private Smart Grid; LC-SC3-EC-4-2020, EVIDENT: Behavioral Insgihts and Effective Energy Policy Actions; ICT-56-2020, TERMINET: Next Generation Smart Interconnected IoT; and HORIZON-JU-SNS-2022-STREAM-A-01-06, NANCY: An Artificial Intelligent Aided Unified Network for Secure Beyond 5G Long Term Evolution, while he also coordinates the Operational Program MARS: Smart Farming With Drones (Competitiveness, Entrepreneurship, and Innovation) and the Erasmus+ KA2 ARRANGE-ICT: SmartROOT: Smart Farming Innovation Training. He serves as a Technical Manger of the H2020-DS-04-2020, ELECTRON: Resilient and Self-Healed Electrical Power Nanogrid, while he served as a Principal Investigator in the H2020-DS04-2018, SDN-microSENSE: SDN-microgrid Resilient Electrical Energy System and in three Erasmus+ KA2, namely, ARRANGE-ICT: Partnership for Addressing Megatrends in ICT; JAUNTY: Joint Undergraduate Courses for Smart Energy Management Systems; and STRONG: Advanced First Responders Training (Cooperation for Innovation and the Exchange of Good Practices). He participates in the editorial boards of various journals.

**DAVID PLETS** (Member, IEEE) has been a member of the imec-WAVES Group, Department of Information Technology (INTEC), Ghent University since 2006, where he has also been a Professor since 2016. His current research interests include localization techniques and IoT, for industrial, agricultural, and healthcare applications. He is also involved in the optimization of wireless communication networks

**WOUT JOSEPH** (Senior Member, IEEE) was born in Ostend, Belgium, on 21 October 1977. He received the M.Sc. degree in electrical engineering from Ghent University, Belgium, in July 2000, and the Ph.D. degree in March 2005; this work dealt with measuring and modeling of electromagnetic fields around base stations for mobile communications related to the health effects of the exposure to electromagnetic radiation. He was a Postdoctoral Fellow with the FWO-V (Research Foundation—Flanders) from 2007 to 2012. Since October 2009, he has been a Professor in the domain of "Experimental Characterization of wireless communication systems." He has been an IMEC PI since 2017. His professional interests are electromagnetic field exposure assessment, propagation for wireless communication systems, antennas and calibration. Furthermore, he specializes in wireless performance analysis and quality of experience.

**SHAOHUA WAN** (Senior Member, IEEE) received the Ph.D. degree from the School of Computer, Wuhan University, Wuhan, China, in 2010. He is currently a Full Professor with the Shenzhen Institute for Advanced Study, University of Electronic Science and Technology of China, Shenzhen, China. From 2016 to 2017, he was a Visiting Professor with the Department of Electrical and Computer Engineering, Technical University of Munich, Munich, Germany. He is the author of more than 150 peer-reviewed research papers and books, including more than 50 IEEE/ACM Transactions papers, such as IEEE TRANSACTIONS ON MOBILE COMPUTING, IEEE TRANSACTIONS ON WIRELESS COMMUNICATIONS, IEEE TRANSACTIONS ON COMMUNICATIONS, IEEE TRANSACTIONS ON INTELLIGENT TRANSPORTATION SYSTEMS, *ACM Transactions on Internet Technology*, IEEE TRANSACTIONS ON NETWORK SCIENCE AND ENGINEERING, IEEE TRANSACTIONS ON NETWORK AND SERVICE MANAGEMENT, IEEE TRANSACTIONS ON MULTIMEDIA, *ACM Transactions on Embedded Computing Systems*, *ACM Transactions on Multimedia Computing, Communications, and Applications*, IEEE TRANSACTIONS ON AUTOMATION SCIENCE AND ENGINEERING, and many top conference papers in the fields of edge intelligence. His research interests mainly include deep learning for intelligent transportation systems.

**CHRISTOS G. CHRISTODOULOU** (Life Fellow, IEEE) received the Ph.D. degree in electrical engineering from North Carolina State University in 1985.

He is currently with the Department of Electrical and Computer Engineering, The University of New Mexico, where he serves as the Director of COSMIAC (Research Center on Space Electronics). He has published over 600 papers in journals and conferences, written 19 book chapters, coauthored nine books, and has several patents. Over his academic career, he has served as the major advisor for over 40 Ph.D. and 75 M.S. students.

Dr. Christodoulou is the recipient of the 2010 IEEE John Krauss Antenna Award for his work on reconfigurable fractal antennas using MEMS switches and has been inducted in the Alumni Hall of Fame for the Electrical and Computer Engineering Department, North Carolina State University in 2016. He was appointed as an IEEE AP-S Distinguished Lecturer from 2007 to 2010 and served as an Associate Editor for the IEEE TRANSACTIONS ON ANTENNAS AND PROPAGATION for six years. He served as the Co-Editor for a special issue on "Reconfigurable Systems" in the IEEE Proceedings in March 2015, the Co-Editor of the IEEE Antennas and Propagation Special issue on "Synthesis and Optimization Techniques in Electromagnetics and Antenna System Design" in March 2007, and for the Special issue on "Antenna Systems and Propagation for Cognitive Radio" in 2014. Since 2013, he has been serving as the Series Editor for Artech House Publishing Company for the areas of antennas, propagation, and electromagnetics. He is a member of Commission B of the U.S. National Committee for URSI and a Distinguished Professor at UNM.

**GEORGE K. KARAGIANNIDIS** (Fellow, IEEE) is currently a Professor with the Electrical and Computer Engineering Department, Aristotle University of Thessaloniki, Greece. He is also a Faculty Fellow with the Cyber Security Systems and Applied AI Research Center, Lebanese American University. His research interests are in the areas of wireless communications systems and networks, signal processing, optical wireless communications, and wireless power transfer and applications. He has received three prestigious awards: The 2021 IEEE ComSoc RCC Technical Recognition Award, the 2018 IEEE ComSoc SPCE Technical Recognition Award, and the 2022 Humboldt Research Award from Alexander von Humboldt Foundation. He is one of the highly-cited authors across all areas of Electrical Engineering, recognized from Clarivate Analytics as Web-of-Science a Highly-Cited Researcher in the eight consecutive years from 2015 to 2022. He was the past editor in several IEEE journals and from 2012 to 2015 he was the Editor-in Chief of IEEE COMMUNICATIONS LETTERS. From September 2018 to June 2022, he served as an Associate Editor-in-Chief for IEEE OPEN JOURNAL OF COMMUNICATIONS SOCIETY.

**SOTIRIOS K. GOUDOS** (Senior Member, IEEE) received the B.Sc. degree in physics, the M.Sc. degree in electronics, and the Ph.D. degree in physics from the Aristotle University of Thessaloniki in 1991, 1994, and 2001, respectively, the master's degree in information systems from the University of Macedonia, Greece, in 2005, and the Diploma degree in electrical and computer engineering from the Aristotle University of Thessaloniki, in 2011. He joined the Department of Physics, Aristotle University of Thessaloniki in 2013, where he is currently an Associate Professor. He is the Director of the ELEDIA@AUTH Laboratory and a member of the ELEDIA Research Center Network. He is the author of the book "*Emerging Evolutionary Algorithms for Antennas and Wireless Communications*", (Institution of Engineering and Technology, 2021). His research interests include antenna and microwave structure design, evolutionary algorithms, wireless communications, and semantic Web technologies. He is the founding Editor-in-Chief of the *Telecom* (MDPI). He currently serves as an Associate Editor for IEEE TRANSACTIONS ON ANTENNAS AND PROPAGATION, IEEE ACCESS, and IEEE OPEN JOURNAL OF THE COMMUNICATION SOCIETY. He is currently serving as the IEEE Greece Section Vice-Chair.